

Supporting Information

A Nonheme, High-Spin $\{\text{FeNO}\}^8$ Complex that Spontaneously Generates N_2O

Alex M. Confer,[†] Alison C. McQuilken,[†] Hirotoshi Matsumura,[‡] Pierre Moënne-Loccoz,^{,†} and David P. Goldberg^{*,†}*

[†]Department of Chemistry, Johns Hopkins University, Baltimore, Maryland, 21218, United States

[‡]Institute of Environmental Health, Oregon Health & Science University, Portland, Oregon, 97239, United States

Contents

General procedures	S3
Physical methods	S3-S4
Synthesis of $[\text{Fe}^{\text{II}}(\text{N}_3\text{PyS})(\text{CH}_3\text{CN})]\text{BF}_4$ (2)	S4-S5
UV-vis titration of 1 with CoCp_2^* at -40 °C	S5
UV-vis titration of 3 with $[\text{FeCp}_2]^+\text{PF}_6^-$ at -40 °C	S5-S6
Cyclic voltammogram of 1 in CH_3CN (Figure S1)	S6
UV-vis spectra: 3 + $[\text{FeCp}_2]^+\text{PF}_6^-$ titration (Figures S2-S4)	S7-S8
EPR characterization of $\{\text{FeNO}\}^8$ complex 3	S8
EPR spectra of 1 and 3 (Figure S5)	S9
Solution magnetic moment of $\{\text{FeNO}\}^8$ complex 3	S9-S10
$^1\text{H-NMR}$ spectrum: Evans method measurement for 3 (Figure S6)	S10
Resonance Raman (RR) characterization of 3	S11
Resonance Raman (RR) spectra of 3 (low frequency region, Figure S7)	S12
Headspace gas chromatography (GC) measurements	S13
Authentic N_2O standard from $\text{H}_2\text{N}_2\text{O}_2$ decomposition	S13-S14
N_2O formation by 3 . Headspace GC	S14-S15
N_2O yield for the reaction of 3 + $[\text{Me}_3\text{NH}]^+[\text{BPh}_4]^-$	S15
Headspace gas chromatography (GC) traces (Figures S8-S9)	S16
UV-vis reaction of 2 + Piloty's acid + $^t\text{BuOK}$ / 18C6 at -40 °C in CH_3CN	S17
UV-vis reaction of 2 + Piloty's acid + $^t\text{BuOK}$ / 18C6 at -80 °C in $\text{C}_3\text{H}_7\text{CN}$	S17-S18
UV-vis spectrum: reactivity of 2 + Piloty's acid at -80 °C (Figure S10)	S18
DFT computational studies (Tables S1-S3)	S19-S22
Spin density plot for ${}^3[\text{Fe}(\text{NO})(\text{N}_3\text{PyS})]$ (Figure S11)	S22
Unrestricted corresponding orbital (UCO) diagrams (Figures S12-S13)	S23-S25
Analytical frequency calculations for 1 and 3	S26-S38
DFT initial guess coordinates and geometry optimized structures	S39-S46
References	S47

General Procedures. All syntheses and manipulations were conducted in an N₂-filled glovebox (Vacuum Atmospheres, O₂ < 0.2 ppm, H₂O < 0.5 ppm) or using standard Schlenk techniques under an atmosphere of Ar unless otherwise noted. All reagents were purchased from commercial vendors and used without further purification unless otherwise noted. Potassium *tert*-butoxide ('BuOK, sublimed grade, 99.99% trace metals basis) was purchased from Sigma-Aldrich and stored in the glovebox. Silver hyponitrite (Ag₂N₂O₂) was prepared from sodium *trans*-hyponitrite hydrate (Na₂N₂O₂ • xH₂O) according to a literature procedure.¹ Acetonitrile, acetonitrile-*d*₃, toluene, toluene-*d*₈, and hexamethyldisiloxane were distilled from CaH₂. Butyronitrile was distilled from Na₂CO₃ / KMnO₄ according to a literature procedure.² Diethyl ether was obtained from a PureSolv solvent purification system (SPS) and used without further purification. All solvents were degassed by a minimum of three freeze-pump-thaw cycles and stored over freshly activated 3 Å molecular sieves in the glovebox. Nitric oxide gas was purchased from Matheson gases, purified according to a literature procedure,³ and stored in a dry, sealed Schlenk flask until use. ¹⁵N¹⁸O (>98% ¹⁵N, > 95% ¹⁸O) gas was purchased from Isotec and used without further purification. Bis(pentamethylcyclopentadienyl)cobalt(II) (CoCp*₂) was purified by recrystallization from a cold saturated hexamethyldisiloxane solution,⁴ or from a cold saturated heptane solution, and stored in the dark under an inert atmosphere prior to use. The thioether ligand N3PySR (R = -CH₂CH₂CN), the Fe^{II}-thioether complex [Fe^{II}(N3PySR)(CH₃CN)](BF₄)₂, and the {FeNO}⁷ complex [Fe(NO)(N3PyS)]BF₄ (**1**) were prepared as previously reported.⁵⁻⁷

Physical Methods. UV-visible spectra were recorded on a Varian Cary 50 Bio spectrophotometer equipped with a Unisoku USP-203 cryostat. NMR spectra were recorded on a Bruker Avance 400 MHz FT-NMR spectrometer at 25 °C. Electron paramagnetic resonance (EPR) spectroscopy was performed on a Bruker EMX spectrometer controlled with a Bruker ER 041 X

G microwave bridge and equipped with a continuous-flow liquid helium cryostat (ESR900) coupled to an Oxford Instruments TC503 temperature controller. The EPR spectra were obtained at 15 K under nonsaturating microwave power conditions (ν = 9.475 GHz, microwave power = 0.201 mW, modulation amplitude = 10 G, modulation frequency = 100 kHz). Headspace gas chromatography (GC) measurements were performed on a Varian CP-3800 instrument equipped with a 1041 injector, electron capture detector, and molecular sieve capillary column. Grade 5.0 nitrogen was used as both the carrier (8 mL/min) and the make-up (22 mL/min) gas. For all measurements, the column oven temperature was kept constant at 150 °C. The injector oven was held at 200 °C, and the detector oven was held at 300 °C.

Synthesis of $[\text{Fe}^{\text{II}}(\text{N3PyS})(\text{CH}_3\text{CN})]\text{BF}_4$ (2). Complex **2** was prepared by on-metal deprotection of the Fe^{II} -thioether precursor with $^{\prime}\text{BuOK}$ in a modification of the previously reported synthesis.⁵ Crystalline $[\text{Fe}^{\text{II}}(\text{N3PySR})(\text{CH}_3\text{CN})](\text{BF}_4)_2$ (99.1 mg, 0.137 mmol) was dissolved in CH_3CN (8 mL) with vigorous stirring to afford a dark red-orange solution. To this solution, a slurry of $^{\prime}\text{BuOK}$ (16.3 mg, 0.145 mmol) in CH_3CN (2 mL) was added dropwise over 2 min, resulting in a rapid color change to deep red. The dark red mixture was stirred for 6 h, then filtered through a celite plug to remove precipitates. Removal of the CH_3CN *in vacuo* afforded deprotected $[\text{Fe}^{\text{II}}(\text{N3PyS})(\text{CH}_3\text{CN})]\text{BF}_4$ as a dark red solid, which was washed with copious amounts of Et_2O . The crude material was dissolved in a mixture of $\text{CH}_3\text{CN}/\text{toluene}$ (1/1 v/v, 4 mL), filtered through a Celite plug, and precipitated as a free-flowing dark red solid by addition of a large excess of cold Et_2O . Isolation of the red solid by filtration followed by drying *in vacuo* gave **2** as a dark red solid. Yield: 46.0 mg (58 %). Earlier attempts at precipitation of **2** by addition of Et_2O to pure CH_3CN resulted in dramatically lower yields because of the high solubility of **2** in

CH_3CN . An equal volume of toluene was added to reduce this solubility. $^1\text{H-NMR}$ and UV-vis spectra matched those previously reported.

Titration of $[\text{Fe}(\text{NO})(\text{N}3\text{PyS})]\text{BF}_4$ (1) with decamethylcobaltocene at -40 °C. An amount of crystalline **1** (1.7 mg, 3.0 μmol) was dissolved in CH_3CN (6.7 mL), and an aliquot of the resulting solution (0.5 mL, 0.22 μmol) was diluted to a final volume of 2.0 mL (0.11 mM) inside of a Schlenk cuvette that was equipped with a micro stir-bar and sealed with a rubber septum. A stock solution of CoCp^*_2 in toluene (4.4 mM) was prepared by dissolving an amount of crystalline CoCp^*_2 (2.9 mg, 8.8 μmol) in toluene (2 mL). The cuvette containing **1** was then cooled to -40 °C in the cryostat attached to the UV-vis spectrophotometer, and the CoCp^*_2 solution was carefully added to **1** in 10 μL increments (0.044 μmol , 0.2 equiv) *via* gas-tight syringe with stirring. Isosbestic conversion to the $\{\text{FeNO}\}^8$ complex **3** ($\lambda_{\max} = 520, 720$ nm) was observed, with isosbestic points at 334 and 470 nm. Maximum formation of **3** was observed upon addition of 1.0 equiv of CoCp^*_2 .

Titration of 3 with $[\text{FeCp}_2]^+\text{PF}_6^-$ at -40 °C. An amount of crystalline **1** (1.4 mg, 2.5 μmol) was dissolved in CH_3CN (5.6 mL), and an aliquot of the resulting solution (0.5 mL, 0.22 μmol) was diluted to 2.0 mL (0.11 mM) inside of a Schlenk cuvette that was equipped with a micro stir-bar and sealed with a rubber septum. A stock solution of $[\text{FeCp}_2]^+\text{PF}_6^-$ (4.2 mM) was prepared by dissolving an amount of solid $[\text{FeCp}_2]^+\text{PF}_6^-$ (3.8 mg, 11 μmol) in CH_3CN (2.6 mL). The cuvette containing **1** was then cooled to -40 °C in the cryostat attached to the UV-vis spectrophotometer and titrated with CoCp^*_2 (1 equiv) until maximum formation of the $\{\text{FeNO}\}^8$ complex **3** was observed. The $[\text{FeCp}_2]^+\text{PF}_6^-$ solution was then carefully added to **3** in 10 μL increments (0.042 μmol , 0.2 equiv) *via* gas-tight syringe with continued stirring. Isosbestic re-oxidation to the $\{\text{FeNO}\}^7$ complex **1** was observed, with retention of one isosbestic point at 470 nm. The second

isosbestic point at 334 nm is likely obscured by absorbance from FeCp₂. Complete recovery of the spectrum for **1** was observed upon addition of 1.1 – 1.2 equiv [FeCp₂]⁺PF₆⁻, confirming the chemical reversibility of the {FeNO}^{7/8} couple at -40 °C. Further addition of [FeCp₂]⁺PF₆⁻ resulted in diminution of the {FeNO}⁷ feature at 440 nm.

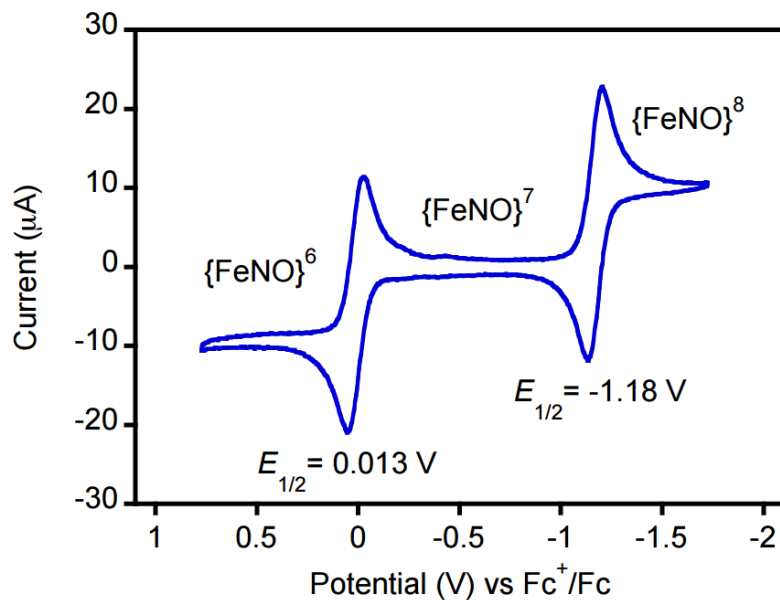


Figure S1. Cyclic voltammogram of a 1.5 mM solution of **1** in CH₃CN with 0.1 M TBAPF₆ as supporting electrolyte, scan rate 50 mV/s. (Reproduced from *J. Am. Chem. Soc.* **2013**, *135*, 14024-7)

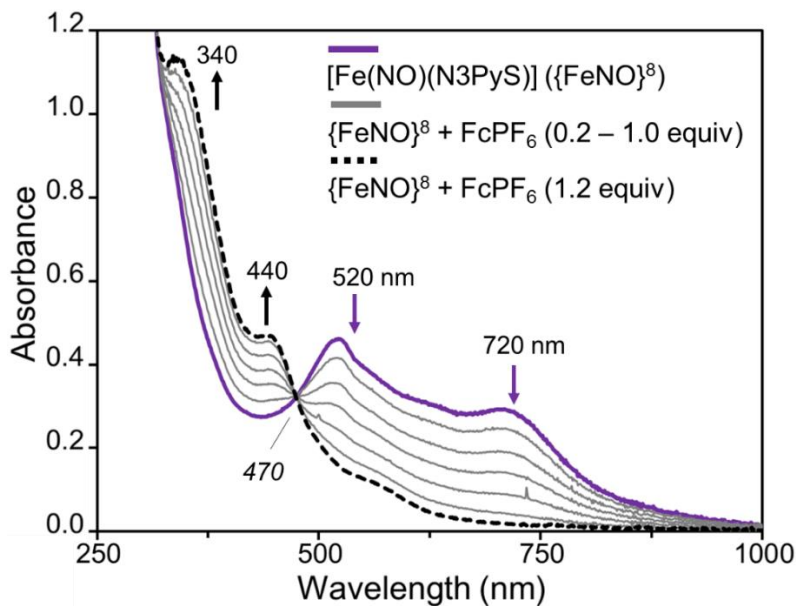


Figure S2. UV-vis spectral titration showing the one-electron re-oxidation of $[\text{Fe}(\text{NO})(\text{N3PyS})]$ (**3**) (purple line) to $[\text{Fe}(\text{NO})(\text{N3PyS})]^+$ (**1**) (black dashed line) upon addition of $[\text{FeCp}_2]^+\text{PF}_6^-$ (0.2 – 1.2 equiv) in $\text{CH}_3\text{CN}/\text{toluene}$ at -40°C . The isosbestic point at 470 nm, also seen in the reduction of **1** to **3**, is retained during the re-oxidation reaction.

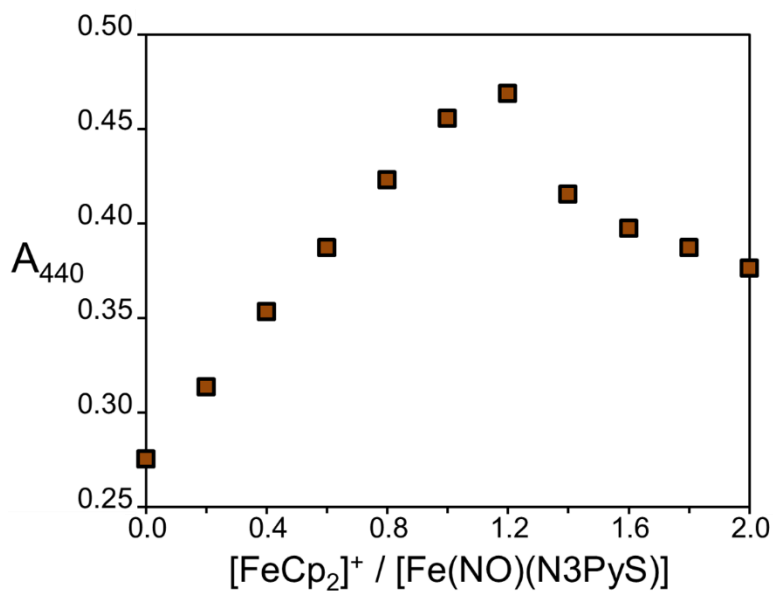


Figure S3. Plot of absorbance at 440 nm, the peak corresponding to the $\{\text{FeNO}\}^7$ complex **1**, versus the ratio of added $[\text{FeCp}_2]^+$ to **3**. Re-oxidation of **3** to **1** is complete upon addition of 1.2 equiv of $[\text{FeCp}_2]^+$. The band at 440 nm diminishes for ratios larger than 1.2, consistent with some decay caused by over-oxidation.

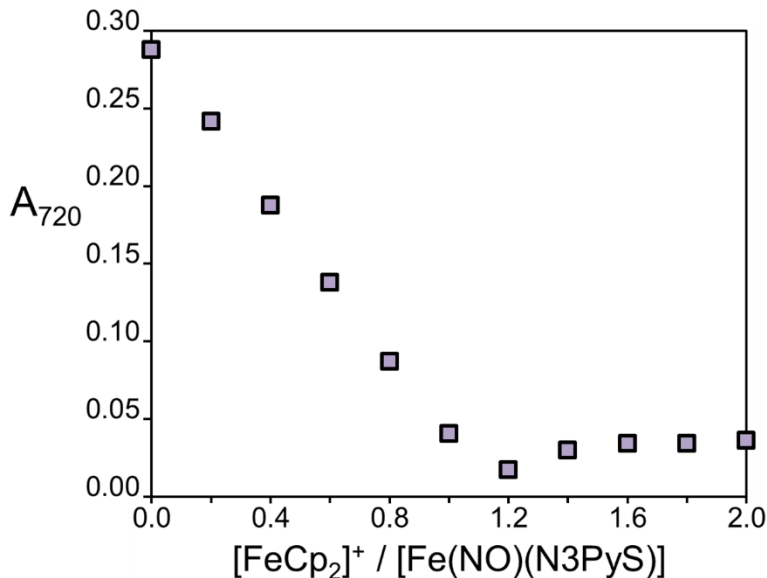


Figure S4. Plot of absorbance at 720 nm, the peak corresponding to the {FeNO}⁸ complex **3**, versus the ratio of added [FeCp₂]⁺ to **3**. Re-oxidation of **3** to **1** is complete upon addition of 1.2 equiv of [FeCp₂]⁺.

Characterization of {FeNO}⁸ complex **3 by EPR spectroscopy.** Under reduced light, a stock solution of {FeNO}⁷ complex **1** in CH₃CN (2.9 mM) was prepared by dissolving an amount of crystalline **1** (2.5 mg, 4.4 μmol) in CH₃CN (1.5 mL). A stock solution of CoCp^{*}₂ in toluene (3.1 mM) was prepared by dissolving an amount of crystalline material (4.1 mg, 12 μmol) in toluene (4 mL) with vigorous stirring. An aliquot of the CoCp^{*}₂ solution (200 μL, 0.62 μmol) was added to an aliquot of **1** (200 μL, 0.58 μmol), producing an intense purple color. The reaction mixture was quickly transferred to a 4 mm quartz EPR tube, which was capped with a septum and frozen by slow annealing in liquid nitrogen prior to collecting spectra at 15 K. The intense signal observed for low-spin **1** (*S* = 1/2), centered at *g* 2.007, disappears completely upon one-electron reduction, resulting in EPR-silent **3**. A residual EPR signal near *g* 2.00 can be assigned to unreacted CoCp^{*}₂ (Co^{II}, *d*⁷, *S* = 1/2).

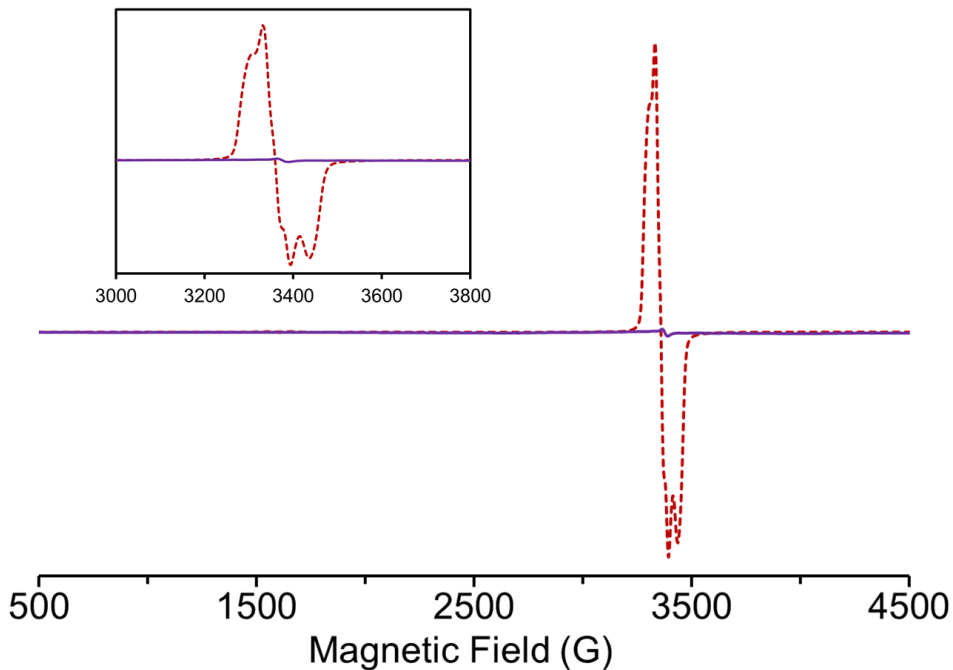


Figure S5. EPR spectra of **1** (red dashed line) and **3** (purple line). Inset: Expanded region near g 2.00.

Evans method solution magnetic moment of $\{\text{FeNO}\}^8$ complex **3.** A stock solution of protio-toluene in CD_3CN (9% toluene) was prepared by mixing 50 μL of toluene in 500 μL of CD_3CN . An aliquot of the toluene stock solution (75 μL) was syringed into a glass capillary that was flame sealed and inserted into a screw-top NMR tube. A stock solution was prepared by dissolving an amount of CoCp^*_2 (7.1 mg, 22 μmol) in toluene (500 μL) with vigorous stirring to give a final concentration of 43.1 mM. Under reduced light, an amount of **1** (1.2 mg, 2.0 μmol) was dissolved in CD_3CN (600 μL), and to this solution was added an aliquot of the CoCp^*_2 stock solution (50 μL , 2.0 μmol , 1 equiv), resulting in an immediate color change from brown to purple indicating formation of the $\{\text{FeNO}\}^8$ complex **3** (final concentration of **3**: 3.1 mM). The reaction mixture was quickly transferred to the NMR tube containing the sealed toluene capillary, and ^1H -NMR spectra were recorded.

The chemical shift of the singlet assigned to the -CH₃ peak for toluene in the presence of the paramagnetic complex was compared to that of the same peak in the capillary insert. The effective spin-only magnetic moment was calculated by simplified Evans method⁸ using the equation $\mu_{\text{eff}} = 0.0618(\Delta v T / 2fM)^{1/2}$, where f is the oscillator frequency (MHz) of the superconducting spectrometer, T is the temperature (K), M is the molar concentration of the paramagnetic metal complex, and Δv is the difference in frequency (Hz) between the two reference toluene -CH₃ signals. The number of unpaired electrons (n) was calculated using the following equation, $\mu_{\text{eff}}^2 = n(n+2)$. The data in Figure S6 give $\Delta v = 18.81$ Hz, $\mu_{\text{eff}} = 2.9 \mu_B$.

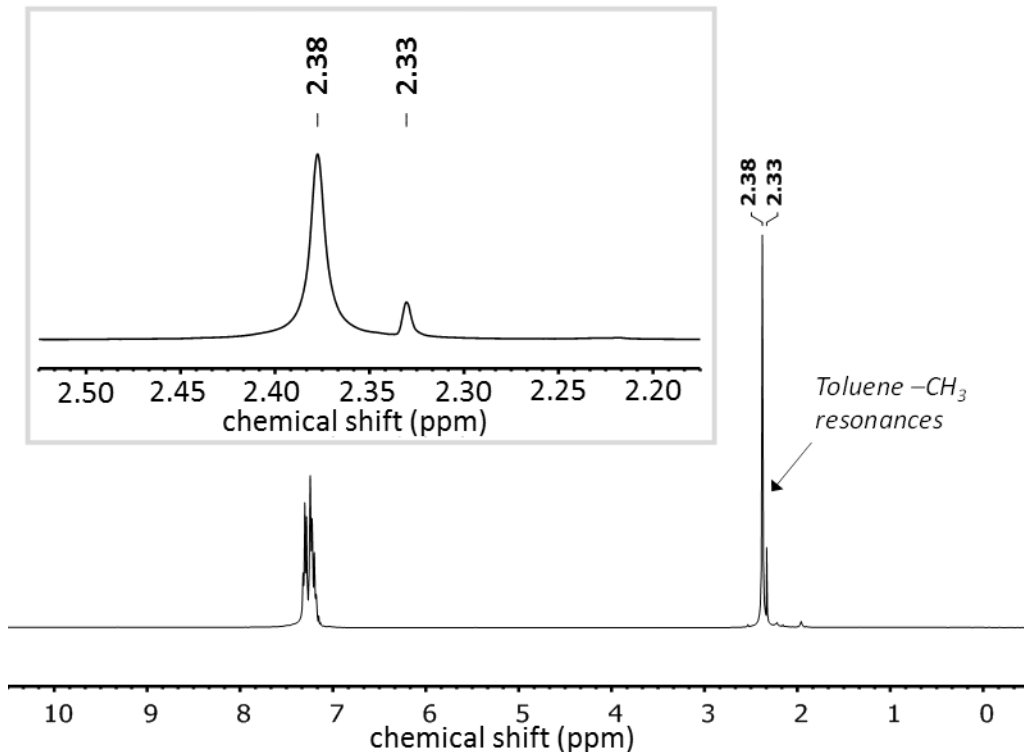


Figure S6. Evans method determination of the solution magnetic moment for **3** (0.0032 M), generated *in situ* by the reaction of **1** with CoCp₂^{*} (1 equiv) in CD₃CN/toluene. Difference in frequency between toluene -CH₃ reference signals, $\Delta v = 18.81$ Hz; f = 400.13 MHz; T = 297.7 K.

Resonance Raman (RR) characterization of **3.** Under reduced light, an amount of **1** (2.5 mg, 4.4 μ mol) was dissolved in CD₃CN (0.8 mL). To this solution was added an aliquot of CoCp^{*}₂ (1 equiv) suspended in toluene (45 μ L), resulting in an immediate color change from dark brown to deep purple indicating reduction of **1** to the {FeNO}⁸ complex **3**. The final concentration of the Fe complex was 5.2 mM. An aliquot of the reaction mixture (0.4 mL) was quickly transferred to a Wilmad-WG-5MM-ECONOMY-9 NMR tube, which was capped with a septum, removed from the glovebox, and frozen in N₂ (l) within ~2 min of the initial mixing. The **3**-¹⁵N¹⁸O isotopologue was prepared in an identical manner from crystalline **1**-¹⁵N¹⁸O. RR spectra were recorded with a McPherson 2061/207 spectrograph equipped with variable gratings and with a liquid nitrogen cooled CCD detector (LN-1100PB, Princeton Instruments). The 458 nm laser emission from an Ar laser (Innova 90, Coherent) was used for enhancement of the {FeNO}⁷ complex **1**, while the 647 nm emission from a Kr laser (Innova 300, Coherent) preferentially enhanced the {FeNO}⁸ complex **3**. Data acquisition was performed using a back-scattering geometry on samples maintained at 110 K inside a copper rod dipped in liquid nitrogen. Long-pass filters (RazorEdge, Semrock) were used to attenuate the Rayleigh scattering. Rapid acquisitions with minimal laser power on spinning samples were compared with longer acquisition time on static samples to assess the photosensitivity of the complexes. Frequencies were calibrated relative to CCl₄ and aspirin and are accurate to $\pm 1\text{cm}^{-1}$.

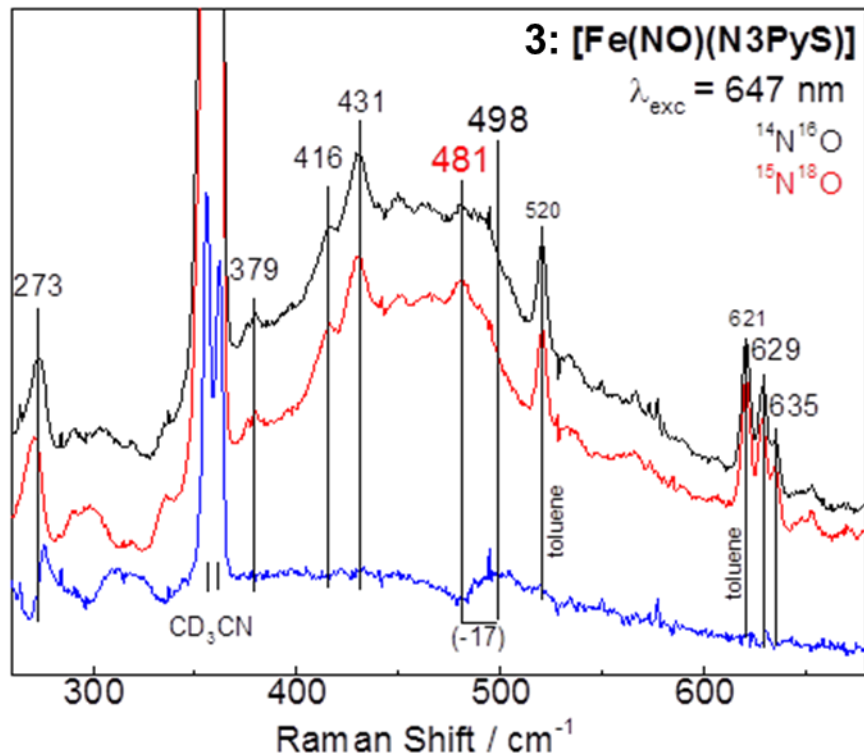


Figure S7. Resonance Raman spectra of **3** (low frequency region) with ¹⁴N¹⁶O (black) and ¹⁵N¹⁸O (red) obtained with a 647 nm excitation on samples maintained at 110 K; the isotopic difference spectrum is also shown (blue). The two spectra were normalized relative to the 629 and 635 cm^{-1} doublet originating from the ligand (N₃PyS); residual contributions to the difference spectrum from CD₃CN are assigned to minor differences in CD₃CN:toluene solvent ratio during the preparation of the {FeNO}⁸ species.

Headspace gas chromatography (GC) measurements. All samples were prepared under N₂ atmosphere in glass headspace vials (Wheaton, 6 mL) equipped with a rubber septum and 20 mm aluminum seals. After preparing each sample, the vial was sealed using a mechanical crimper, wrapped in aluminum foil (to exclude ambient light) unless otherwise noted, and allowed to incubate at 23 °C for the amount of time specified. An aliquot of the headspace above the sample solution (60 µL) was pulled into a gas-tight glass syringe (100 µL) with a two-way sample locking mechanism. The headspace aliquot was then injected into the GC. The method chosen for N₂O detection had a characteristic column retention time of 6.7 min for N₂O, and a retention time of 1.3 min for residual air from the syringe. At approximately 1 and 2 min after the initial injection, two additional 60 µL headspace aliquots were injected into the GC to provide a total of three trials, with a constant retention time difference of 5.4 min between the residual air peak and the N₂O peak for each trial. The three N₂O peaks were manually integrated using the GC software and averaged.

Authentic N₂O standard from H₂N₂O₂ decomposition. The total amount of N₂O partitioned between the solution and headspace is proportional to the area under the characteristic N₂O peak and can be quantitated by comparison to an authentic standard, provided that the two samples have similar volumes (Equation S1):

$$\frac{\text{Amount of N}_2\text{O (standard)}}{\text{Average N}_2\text{O area (standard)}} = \frac{\text{Amount of N}_2\text{O (sample)}}{\text{Average N}_2\text{O area (sample)}} \quad (\text{Eq. S1})$$

The N₂O yields were determined by comparison to an N₂O standard prepared from hyponitrous acid (H₂N₂O₂) decomposition. HCl reacts with Ag₂N₂O₂ in a 2:1 molar ratio to form H₂N₂O₂ (2 HCl + Ag₂N₂O₂ → H₂N₂O₂ + 2 AgCl), which is unstable and dehydrates with loss of N₂O (H₂N₂O₂ → N₂O + H₂O). Thus, the overall reaction leading to N₂O production is 2 HCl + Ag₂N₂O₂ → N₂O

+ H₂O + 2 AgCl. Since Ag₂N₂O₂ is in excess for these experiments, and assuming that no N₂O is produced from decomposition of Ag₂N₂O₂ in the absence of HCl, the amount of N₂O can therefore be controlled by the HCl limiting reagent.

The H₂N₂O₂ standard was prepared in the following manner. Under reduced light in the glovebox, a headspace vial (Wheaton, 6 mL) was charged with Ag₂N₂O₂ (0.5 mg, 2 µmol) and a micro stir-bar. The Ag₂N₂O₂ was suspended in CH₃CN (2.25 mL), and the vial was sealed. Outside of the glovebox, an amount of anhydrous 2.0 M HCl in Et₂O (100 µL) was diluted with Et₂O to a final volume of 4.1 mL under anaerobic conditions (HCl concentration: 49 mM). With vigorous stirring under reduced light, an aliquot of the dilute HCl solution (10 µL, 0.49 µmol) was added *via* gas-tight syringe to the sealed Ag₂N₂O₂ suspension. The vial was wrapped in aluminum foil to exclude ambient light, and the reaction mixture was stirred at 23 °C for 20 h. The reaction was sampled by headspace GC as described above. Average area of N₂O peaks from three injections: 4358.9 units. N₂O yield: 0.245 µmol.

N₂O formation by 3. Headspace GC. Under reduced light, an amount of **1** (1.2 mg, 2.1 µmol) was dissolved in CH₃CN (5.0 mL). An aliquot of the concentrated {FeNO}⁷ solution (2.6 mL) was diluted with CH₃CN to a final volume of 10.6 mL, and 2.0 mL of this solution was transferred to a headspace vial (Wheaton, 6 mL) equipped with a rubber septum and 20 mm aluminum seal (Fe concentration: 0.10 mM; 0.21 µmol of **1** in the vial). An aliquot of a 2.3 mM CoCp^{*}₂ solution in toluene (100 µL, 0.23 µmol, 1.1 equiv) was added to **1**, producing an immediate color change from brown to purple. The vial was mechanically sealed with a crimper. The {FeNO}⁸ complex (final Fe concentration: 0.095 mM) was allowed to slowly decay by standing in solution for 20 h at 23 °C. The reaction was sampled by headspace GC as described above.

An intense peak for N₂O was observed at the characteristic retention time of 6.7 min for the first injection, and at 7.7 and 8.7 min for the duplicate injections, with an average area of 1000.9 units. Assuming that 1 equiv of N₂O is produced from reductive coupling of 2 equiv of {FeNO}⁸ complex **3** (0.21 μmol), the maximum theoretical yield for this reaction is 0.105 μmol N₂O. From Eq. 1, the total partitioned N₂O was determined to be 0.056 μmol, corresponding to an approximately 54% yield. Control experiments with the {FeNO}⁷ precursor **1** in the absence of reductant showed no N₂O production upon standing in solution (Figure S8).

N₂O yield for the **3 + [Me₃NH]⁺[BPh₄]⁻ reaction.** Under reduced light, an amount of **1** (1.2 mg, 2.1 μmol) was dissolved in CH₃CN (5.0 mL). An aliquot of this solution (2.6 mL) was diluted with CH₃CN to a final volume of 10.6 mL, and 2.0 mL of this solution was transferred to a a headspace vial (Wheaton, 6 mL) equipped with a rubber septum and 20 mm aluminum seal ([**1**] = 0.10 mM; 0.21 μmol of **1** in the vial). An amount of CoCp^{*}₂ (100 μL of a 2.3 mM solution, 0.23 μmol) was added to **1**, producing an immediate color change from brown to purple indicating conversion to **3**. The vial was mechanically sealed with a crimper. Immediately thereafter, an amount of [Me₃NH][BPh₄] (100 μL of a 2.3 mM solution, 0.23 μmol) in CH₃CN was added to **3** via syringe, resulting in a rapid color change from purple to orange-brown. The vial was wrapped in foil and allowed to stand at 23 °C for 20 h. The reaction was sampled by headspace GC as described above. Average area of N₂O peaks from three injections: 73.5 units. N₂O yield: 0.004 μmol (93% decrease in yield relative to **3**).

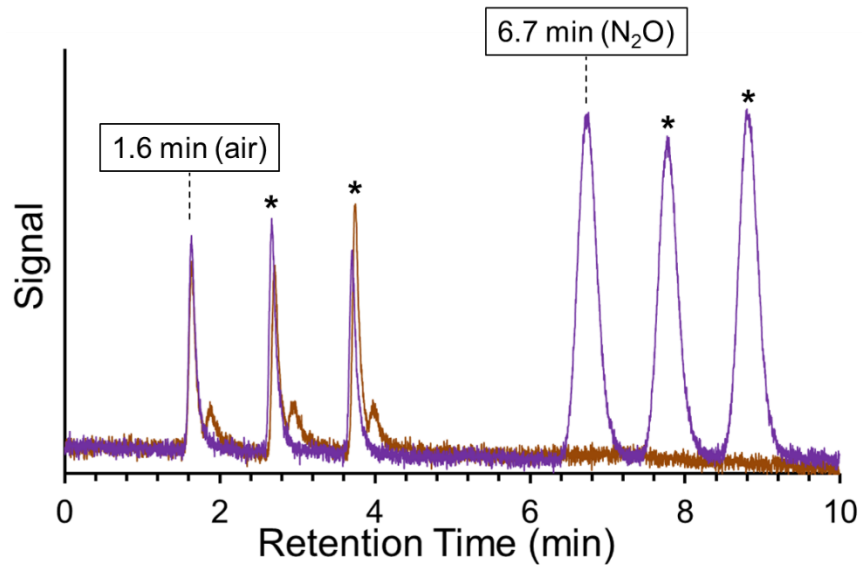


Figure S8. Headspace GC traces for **3** (purple line) and **1** (brown line). Peaks denoted with an asterisk are from duplicate injections at $t = 1$ and 2 min after the initial injection. No N_2O is observed in the headspace above the solution of **1**.

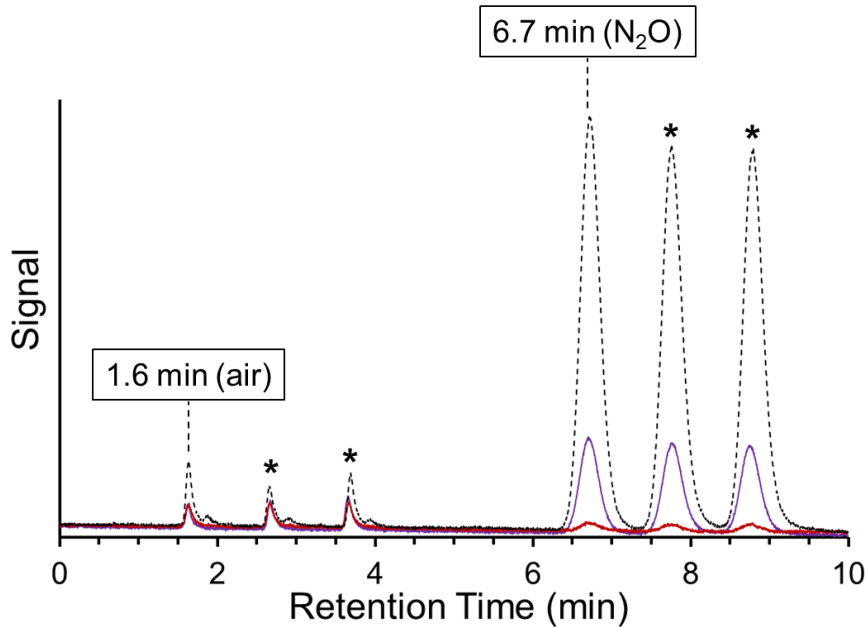


Figure S9. Headspace GC traces for $\text{Ag}_2\text{N}_2\text{O}_2 + \text{HCl}$ (2 equiv) (black dashed line), **3** (purple line) and **3** + $[\text{Me}_3\text{NH}]^+[\text{BPh}_4]^-$ (1 equiv) (red line). Peaks denoted with an asterisk are from duplicate injections at $t = 1$ and 2 min after the initial injection.

Reaction of $[\text{Fe}^{\text{II}}(\text{N3PyS})(\text{CH}_3\text{CN})]\text{BF}_4$ (2**) with Piloty's acid at -40 °C in CH_3CN .** An amount of **2** (1.4 mg, 2.4 μmol) was dissolved in CH_3CN (4 mL), and an aliquot of this stock solution (0.8 mL) was diluted with CH_3CN to a final volume of 4.0 mL in a Schlenk cuvette equipped with a micro stir-bar ($[\mathbf{2}] = 0.12 \text{ mM}$, 0.48 μmol of **2** in the cuvette). The cuvette was sealed with a rubber septum, removed from the glovebox, and cooled to -40 °C with stirring in the cryostat attached to the UV-vis spectrophotometer. To the pre-cooled solution of **2** was added Piloty's acid (100 μL of a 4.9 mM solution in CH_3CN , 0.49 μmol) *via* gas-tight syringe. No change was observed in the UV-vis spectrum for **2**, indicating the absence of a reaction between **2** and Piloty's acid. A solution of 'BuOK / 18-crown-6 in CH_3CN was freshly prepared by dissolving a mixture of 'BuOK (2.3 mg, 20.5 μmol) and 18-crown-6 (6.1 mg, 23.1 μmol) in CH_3CN (4.0 mL) with vigorous stirring. An aliquot of the 'BuOK solution (100 μL , 0.51 μmol , 1.0 equiv) was added slowly *via* gas-tight syringe to the mixture of **2** and Piloty's acid, resulting in loss of the UV-vis bands for **2** ($\lambda_{\text{max}} = 325, 418, 493 \text{ nm}$) over 1 h at -40 °C. The formation of a new species with peaks at 418 and 501 nm was observed, and this new spectrum was stable for at least 6 h at -40 °C. Addition of a second equivalent of 'BuOK at -40 °C resulted in the appearance of the characteristic UV-vis bands for the $\{\text{FeNO}\}^8$ complex **3** at 520 and 720 nm after 5 min. Complex **3** generated by this method has limited stability and fully decays within 10 min at -40 °C.

Reaction of $[\text{Fe}^{\text{II}}(\text{N3PyS})(\text{CH}_3\text{CN})]\text{BF}_4$ (2**) with Piloty's acid at -80 °C in $\text{C}_3\text{H}_7\text{CN}$.** An amount of **2** (1.5 mg, 2.6 μmol) was dissolved in $\text{C}_3\text{H}_7\text{CN}$ (5.9 mL), and an aliquot of this stock solution (0.5 mL) was diluted with $\text{C}_3\text{H}_7\text{CN}$ to a final volume of 2.0 mL in a Schlenk cuvette equipped with a micro stir-bar ($[\mathbf{2}] = 0.11 \text{ mM}$, 0.22 μmol of **2** in the cuvette). The cuvette was sealed with a rubber septum, removed from the glovebox, and cooled to -40 °C with stirring in the cryostat attached to the UV-vis spectrometer. To the pre-cooled solution of **2** was added Piloty's

acid (50 μ L of a 4.5 mM solution in C_3H_7CN , 0.23 μ mol) *via* gas-tight syringe. No change was observed in the UV-vis spectrum for **2**, indicating the absence of a reaction between **2** and Piloyt's acid. A solution of $'BuOK$ / 18-crown-6 in C_3H_7CN was freshly prepared by dissolving a mixture of $'BuOK$ (1.5 mg, 13.4 μ mol) and 18-crown-6 (4.1 mg, 15.5 μ mol) in C_3H_7CN (3.0 mL) with vigorous stirring. An aliquot of the $'BuOK$ solution (50 μ L, 0.22 μ mol, 1.0 equiv) was added slowly *via* gas-tight syringe to the mixture of **2** and Piloyt's acid, resulting in loss of the UV-vis bands for **2** ($\lambda_{max} = 327, 420, 500$ nm) over 20 min at -40 $^{\circ}$ C. The reaction mixture was then cooled to -80 $^{\circ}$ C, and a second equivalent of $'BuOK$ solution was slowly added. The UV-vis bands for **3** were completely formed within 5 min, and no further spectral change was observed for at least 6 h at -80 $^{\circ}$ C.

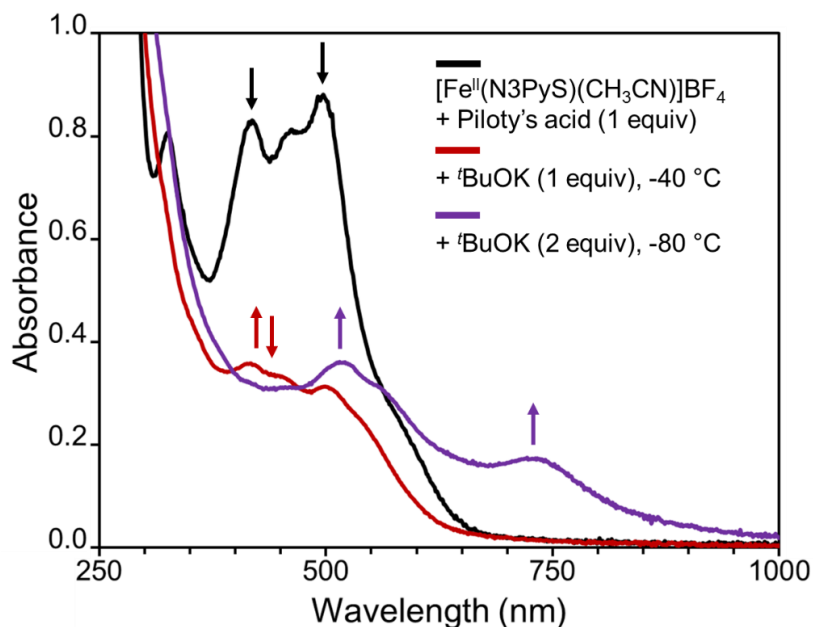


Figure S10. UV-vis spectra showing stepwise addition of $'BuOK$ (1 – 2 equiv) to a pre-mixed solution of **2** and Piloyt's acid (1 equiv) in butyronitrile (C_3H_7CN). The first equiv of $'BuOK$ / 18-crown-6 was added at -40 $^{\circ}$ C to generate the intermediate species (red line), which was cooled to -80 $^{\circ}$ C before the second equiv of $'BuOK$ / 18-crown-6 was added. The spectrum for the $\{FeNO\}^8$ complex **3** (purple line) undergoes no further change for at least 6 h at -80 $^{\circ}$ C.

DFT computational studies. Previous calculations with the pure functional BP86 closely reproduced the experimental crystal structure and S K-edge XAS data of the {FeNO}⁷ complex, [Fe(NO)(N3PyS)]BF₄ (**1**).⁷ For the one-electron reduced {FeNO}⁸ complex, [Fe(NO)(N3PyS)] (**3**), our computational approach involved geometry optimizations at the BP86 level, followed by single point calculations on these optimized structures with the hybrid functional B3LYP to obtain relative energies and spin populations for the singlet ($S = 0$) and triplet ($S = 1$) spin states. This strategy has been used with success for ferrous heme nitrosyl complexes.⁹⁻¹⁰ Although BP86 calculations typically lead to more accurate bond lengths and vibrational frequencies for iron nitrosyl complexes, B3LYP calculations yield more accurate total energies and spin density distributions due to reduced metal-ligand covalency in the Fe-NO unit.¹¹

All calculations were performed in the *ORCA-3.0.3* program package.¹² Fully relaxed geometry optimizations were carried out for **3** in the $S = 0$ and $S = 1$ spin states (denoted ¹{**3**} and ³{**3**}, respectively) using BP86 with the RI approximation and the D3 dispersion correction¹³⁻¹⁴ of Grimme et al. To reduce computational cost, the def2-TZVP basis set¹⁵⁻¹⁶ (triple zeta quality) was implemented for the Fe, S, N, and O atoms (8 atoms total), while the less expensive def2-SVP basis set (double zeta quality) was implemented for the C and H atoms (45 atoms total). The def2-SVP/J auxiliary basis set was applied to all atoms for the RI approximation. The same approach was applied to geometry optimizations for **1** in the $S = \frac{1}{2}$ (²{**1**}) and $S = \frac{3}{2}$ (⁴{**1**}) spin states. Analytical frequency calculations at the same level of theory confirmed that all optimizations had converged to true minima on the potential energy surface (i.e., no imaginary frequencies). Subsequently, single point energy calculations were performed on these optimized structures using B3LYP with the RIJCOSX approximation and the def2-TZVP / def2-TZVP/J basis sets on all atoms. Spin fragments were obtained from the B3LYP Mulliken population analysis. Spin density

and molecular orbital isosurfaces were plotted in UCSF Chimera *1.10* with isosurface values of +/- 0.03 and +/- 0.05 a.u., respectively.¹⁷

Different initial guesses were employed for geometry optimizations of ³{3} and ¹{3}. Starting geometries were obtained by manipulating the single crystal X-ray structure of the {FeNO}⁷ complex [Fe(NO)(N3PyS)]BF₄ (**1**, cation only),⁷ to produce guesses with linear (180°), bent (147°), and strongly bent (120°) Fe-NO units (Table S1). These starting geometries are denoted “Initial Guess A” (**IGA**), “Initial Guess B” (**IGB**), and “Initial Guess C” (**IGC**), respectively. All other bond metrics were unchanged. Using this approach, two distinct minimum energy structures were identified for ³{3} (Table S2). Equivalent structures were obtained for ¹{3} independent of initial guess; however, starting from IGA (linear Fe-NO unit), no optimized structure could be obtained.

Table S1. Comparison of Initial Guess Structures for Geometry Optimizations of ³{3}

Structure	<i>d</i> (Fe-NO)	<i>d</i> (N-O)	<i>d</i> (Fe-N _{eq}), avg	<i>d</i> (Fe-N _{ax})	<i>d</i> (Fe-S)	\angle [Fe-N-O]
IGA	1.733	1.150	2.010	2.130	2.296	179.8
IGB	1.733	1.150	2.010	2.130	2.296	147.2
IGC	1.733	1.150	2.010	2.130	2.296	119.7
* Bond distances in angstroms (Å), bond angles in degrees (°)						

Table S2. BP86 Optimized Structures for ${}^3\{3\}$ and ${}^1\{3\}$

Structure	$d(\text{Fe-NO})$	$d(\text{N-O})$	$d(\text{Fe-N}_{\text{eq}})$, avg	$d(\text{Fe-N}_{\text{ax}})$	$d(\text{Fe-S})$	$\angle [\text{Fe-N-O}]$
${}^3\{3\}\text{-A}$	1.684	1.195	2.121	2.306	2.396	149.4
${}^3\{3\}\text{-B}$	1.686	1.196	2.074	2.247	2.375	147.4
${}^3\{3\}\text{-C}$	1.686	1.196	2.074	2.246	2.374	147.3
${}^1\{3\}\text{-B}$	1.758	1.219	1.957	2.232	2.315	125.5
${}^1\{3\}\text{-C}$	1.758	1.219	1.956	2.234	2.315	125.4
* Bond distances in angstroms (\AA), bond angles in degrees ($^\circ$)						

Whereas **IGB** and **IGC** (both containing bent Fe-NO units) converge to the same optimized geometry (${}^3\{3\}\text{-B/C}$), **IGA** (with a linear Fe-NO unit) converges to a geometry (${}^3\{3\}\text{-A}$) that is $\sim 8.7 \text{ kcal}\cdot\text{mol}^{-1}$ lower in energy. The bond distances for the Fe-NO unit are similar between ${}^3\{3\}\text{-A}$ and ${}^3\{3\}\text{-B/C}$, although the Fe-N-O angle is slightly more linear (149.4°) in ${}^3\{3\}\text{-A}$ as compared to ${}^3\{3\}\text{-B/C}$ (147°). The most significant geometric differences are in the Fe-N distance *trans* to the nitrosyl ligand (0.059 \AA) and in the average of the three Fe-N equatorial distances (0.047 \AA). The Fe-S bond is also slightly elongated in ${}^3\{3\}\text{-A}$ ($+0.021 \text{ \AA}$). Comparison of the Mulliken spin fragments (B3LYP) reveals that the two optimized structures have similar spin distributions (3.1 on Fe, -1.1 on NO) suggestive of an electronic structure that is more in line with hs $\text{Fe}^{\text{I}}\text{-NO}^\bullet$ than hs $\text{Fe}^{\text{II}}\text{-}{}^3\text{NO}^-$ (Table S3). The observation that ${}^3\{3\}\text{-A}$ is $\sim 8.7 \text{ kcal}\cdot\text{mol}^{-1}$ lower in energy than ${}^3\{3\}\text{-B/C}$ could perhaps be attributed to minimized repulsion between the reduced Fe center and the N3PyS donor atoms. The BP86 optimized structure of **3** in the $S = 0$ spin state (${}^1\{3\}$) is $11.8 \text{ kcal}\cdot\text{mol}^{-1}$ higher in energy than the lowest-energy $S = 1$ structure, ${}^3\{3\}\text{-A}$.

Table S3. Mulliken Spin Fragments and Single Point Energies from B3LYP Calculations

	Structure $^3\{3\}\text{-A}$	Structure $^3\{3\}\text{-B}$	Structure $^1\{3\}\text{-B}$
Mulliken spin, Fe	3.156	3.111	0.000
Mulliken spin, S	0.050	0.050	0.000
Mulliken spin, NO	-1.154	-1.102	0.000
Mulliken spin, total	2.000	2.000	0.000
Single point energy (hartree)	-2937.8597	-2937.8459	-2937.8409
Single point energy (kcal mol ⁻¹)	0.0	+8.7	+11.8

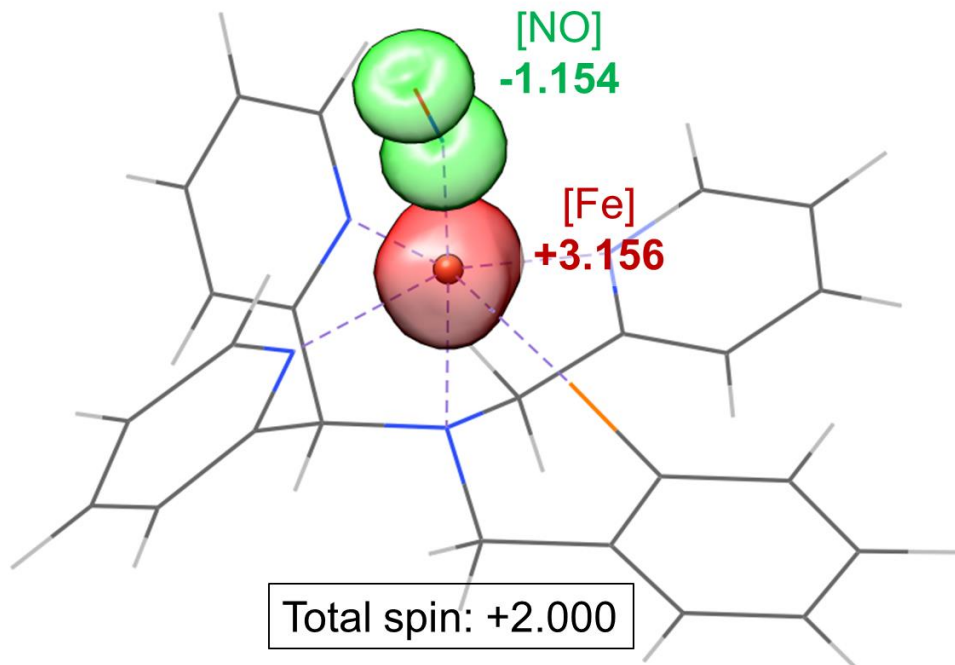


Figure S11. Spin density plot for the triplet ($S = 1$) state of the $\{\text{FeNO}\}^8$ complex, ${}^3\{3\}\text{-B}$, (isosurface value = +/- 0.03 au) showing the unpaired spin distribution within the Fe-NO unit, as obtained from a Mulliken population analysis at the B3LYP level (Table S3).

In order to compare the key frontier MOs for **1** and **3**, unrestricted corresponding orbital (UCO) transformations were performed on the B3LYP calculated MOs. For an arbitrary orbital in the alpha (“spin-up”) manifold, the UCO transformation assigns a corresponding orbital in the beta (“spin-down”) manifold that has the highest degree of spatial overlap. An overlap significantly smaller than one (typically < 0.85) indicates a spin-coupled pair, whereas an overlap closer to one (> 0.85) indicates a doubly occupied MO with some spin polarization.¹⁸ Unpaired electrons are indicated by singly occupied orbitals in the alpha manifold that do not have a corresponding orbital in the beta manifold. The schematic UCO diagrams for **1** and **3** are shown in Figs. S12 and S13, respectively.

The UCO diagram for ⁴{**1**} consists of two spin-coupled pairs of Fe-NO electrons (Fig. S12, MOs $121\alpha\beta$ and $122\alpha\beta$), along with three unpaired electrons in primarily Fe-based alpha orbitals. For the $121\alpha\beta$ and $122\alpha\beta$ pairs, the Fe contributions are greatest in the alpha manifold ($> 82\%$), whereas the NO contributions are greatest in the beta manifold ($> 57\%$). The UCO diagram for one-electron-reduced ³{**3**} indicates that both spin-coupled Fe-NO pairs remain upon reduction (Fig. S13, MOs $122\alpha\beta$ and $123\alpha\beta$). The key difference between ⁴{**1**} and ³{**3**}, however, is the presence of a doubly occupied, Fe-based MO in ³{**3**} (Fig. S13, MO $121\alpha\beta$) that is absent in ⁴{**1**}. The additional electron in ³{**3**} occupies a primarily Fe-based beta orbital and pairs strongly with a singly occupied, Fe-based alpha orbital ($S_{\alpha\beta} = 0.919$), giving rise to an overall $S = 1$ spin state. Thus, the computational analysis supports a mostly metal-centered reduction of **1** to **3**, in line with the findings of Lehnert and Speelman for their hs $[\text{Fe}(\text{NO})(\text{TMG}_3\text{tren})]^{2+/+}$ system.¹⁹

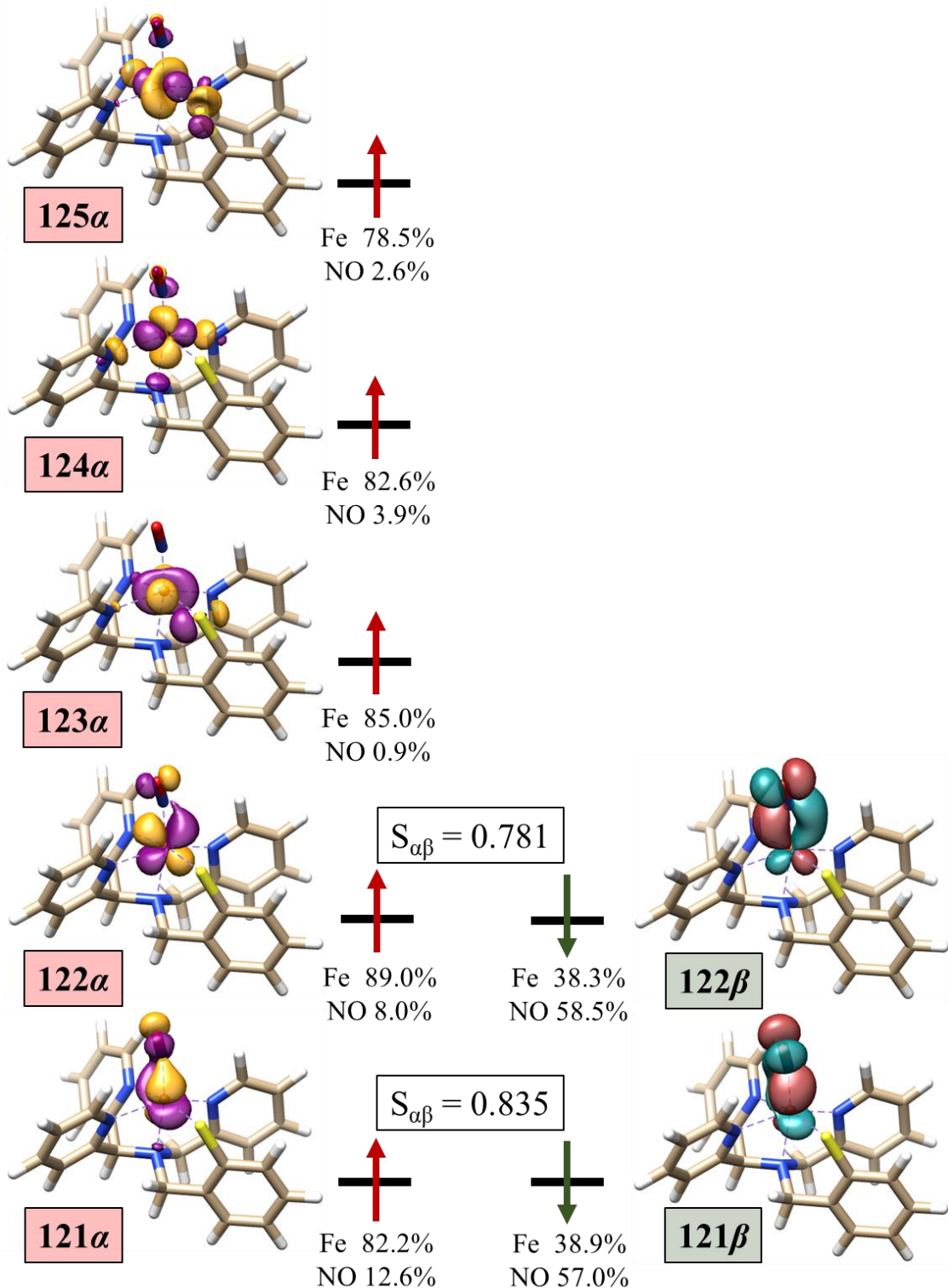
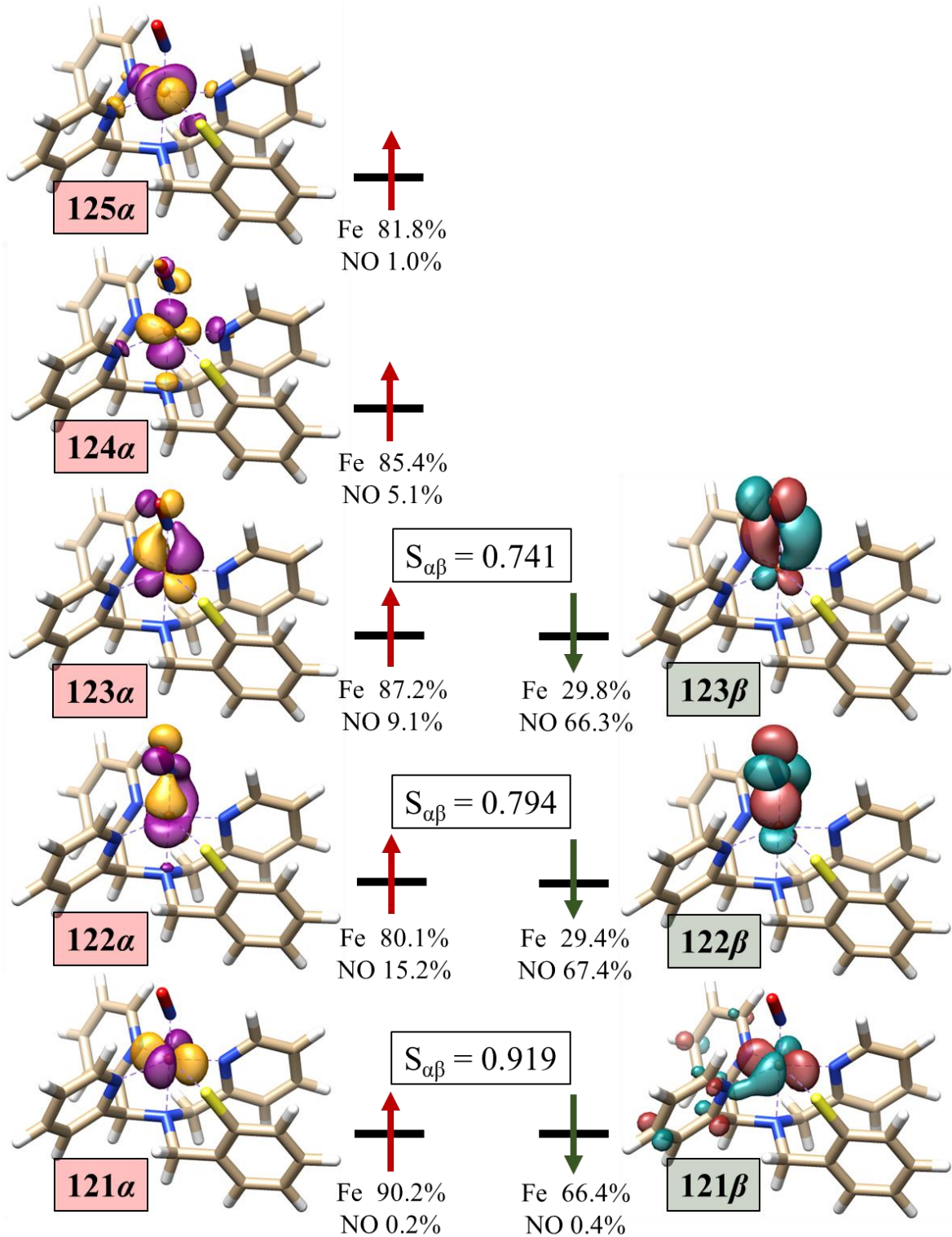


Figure S12. Unrestricted corresponding orbitals for ${}^4\{1\}$ (B3LYP def2-TZVP). $S_{\alpha\beta}$ denotes the degree of spatial overlap between the α and β pair.



Finally, analytical frequency calculations were employed to obtain trends in $\nu(\text{N-O})$ for $^2\{\mathbf{1}\}$, $^4\{\mathbf{1}\}$, $^1\{\mathbf{3}\}$, and $^3\{\mathbf{3}\}$. The results of these calculations are summarized in Table S4.

Table S4. Experimental and Calculated $\nu(\text{N-O})$ for **1** and **3**

	Spin State	$\nu(\text{NO}) (\text{cm}^{-1})$ Expt.	Expt. Method	$\nu(\text{NO}) (\text{cm}^{-1})$ Calc.	Refs.
1	$S = 1/2$	1641	FTIR/RR (CD ₃ CN)	1681	20; this work
1	$S = 3/2$	1737	FTIR (CD ₃ CN)	1724	20
3	$S = 0$	n/a	n/a	1490	this work
3	$S = 1$	1588	RR (CD ₃ CN/toluene)	1643	this work

Although the calculated $\nu(\text{N-O})$ frequency for $^3\{\mathbf{3}\}$ is overestimated by 55 cm⁻¹, a comparable overestimation of 40 cm⁻¹ is observed for $^2\{\mathbf{1}\}$ which suggests that the deviation for $^3\{\mathbf{3}\}$ is reasonable within the errors of the BP86 method. The low calculated $\nu(\text{N-O})$ of 1490 cm⁻¹ for $^1\{\mathbf{3}\}$ further indicates that the 1588 cm⁻¹ RR vibration is unlikely to arise from $^1\{\mathbf{3}\}$. Importantly, DFT predicts a very modest (81 cm⁻¹) decrease in $\nu(\text{NO})$ upon reduction of high-spin **1** ($S = 3/2$) to high-spin **3** ($S = 1$), which is consistent with the UCO analysis and supports a predominantly metal-centered reduction.

Calculated vibrational frequencies for ${}^3\{3\}\text{-A}$ (${}^3\{\text{FeNO}\}^8$)

Mode	freq (cm**-1)	T**2	TX	TY	TZ
6:	42.40	1.927165	(-0.242591	1.346420	0.235516)
7:	49.63	0.330488	(-0.521845	0.198294	0.137278)
8:	55.79	0.175826	(0.075710	-0.033434	-0.411067)
9:	60.37	1.944795	(0.060975	-0.109124	1.388945)
10:	64.41	0.654637	(-0.390854	0.154873	0.691292)
11:	75.25	0.915789	(-0.383204	0.726795	-0.490624)
12:	88.38	0.877469	(0.245089	0.729615	-0.533912)
13:	94.54	1.487731	(0.383915	-0.477820	-1.054527)
14:	107.85	0.631076	(-0.291417	-0.645498	0.359840)
15:	112.16	1.322000	(-0.171913	-0.898746	-0.696206)
16:	115.40	1.286666	(0.401411	1.049763	-0.153410)
17:	133.72	1.840177	(0.238702	-1.077716	-0.788497)
18:	148.53	0.471990	(-0.593880	-0.344924	-0.018024)
19:	176.29	4.261581	(-0.379417	-2.012272	-0.261506)
20:	186.70	2.446590	(-0.732032	0.857353	1.084280)
21:	201.31	0.266149	(-0.447657	-0.207105	0.151194)
22:	218.05	4.397916	(-1.154334	0.748705	1.582678)
23:	219.36	7.380337	(1.220648	-1.723410	-1.708863)
24:	231.41	1.029163	(0.303790	-0.967506	0.028391)
25:	233.13	1.040737	(0.025476	-0.552021	0.857532)
26:	260.39	2.413131	(-0.863045	1.227356	0.402344)
27:	277.87	4.665563	(1.428406	-1.167282	-1.123688)
28:	281.82	1.266762	(0.197375	0.800533	-0.766128)
29:	313.89	2.050738	(-1.040641	-0.968155	-0.174582)
30:	317.44	0.716952	(-0.705243	-0.074588	-0.462623)
31:	321.69	5.474420	(0.631193	-1.880832	-1.240357)
32:	339.71	1.287026	(0.506809	0.900431	0.468396)
33:	383.56	1.862646	(1.253080	0.528011	0.116799)
34:	402.91	8.756329	(-2.185361	-1.760280	-0.939115)
35:	410.41	5.360232	(-0.673924	1.072536	1.937969)
36:	416.98	6.788943	(-1.967057	1.665469	-0.381892)
37:	428.26	2.343447	(-1.478951	-0.390246	-0.062111)
38:	433.03	1.139868	(-0.532945	0.256852	0.888743)
39:	442.39	1.415077	(-0.541279	-0.473444	0.947600)
40:	453.44	1.654686	(0.308285	1.246169	0.081912)
41:	471.62	4.280878	(1.328494	1.004636	-1.227472)
42:	476.78	5.049612	(1.164315	-1.914173	0.172987)
43:	483.73	5.121500	(0.064795	2.196868	-0.539511)
44:	511.99	1.402927	(1.021860	-0.279664	-0.529638)
45:	536.50	1.919763	(-0.776921	-1.129535	0.200768)
46:	555.36	1.373928	(-1.002507	0.574350	0.197559)
47:	596.51	1.460670	(-0.071396	0.921707	-0.778478)
48:	606.06	7.073716	(0.185028	-2.586482	-0.591261)
49:	614.51	6.494666	(-1.989118	-1.269694	-0.962265)
50:	626.77	10.125403	(1.343508	0.407043	-2.855645)
51:	637.03	2.702495	(1.338822	-0.238791	-0.923596)
52:	643.16	4.584241	(-0.767426	-1.788110	0.893285)
53:	683.64	10.841258	(-2.597382	0.703386	1.897396)
54:	686.74	1.980454	(1.341094	-0.236133	-0.355191)
55:	723.26	10.698463	(-2.347587	-0.641153	2.185456)
56:	726.78	15.428868	(-2.254667	-0.906602	3.086004)
57:	730.46	43.819118	(-1.239489	6.325270	-1.507893)
58:	734.30	27.397039	(-3.908385	3.167472	1.445229)
59:	734.94	4.928355	(-0.762770	0.875965	1.891883)
60:	739.02	10.858169	(-1.478783	2.930110	-0.292959)
61:	741.46	6.367905	(0.593063	2.193986	-1.096634)
62:	766.76	6.367773	(-1.299495	0.652576	2.062336)
63:	769.47	7.788585	(1.128686	-0.839867	-2.410244)
64:	822.56	7.139365	(0.603341	-2.598775	0.147351)
65:	830.63	10.777975	(-1.044631	0.342778	3.093416)

66:	847.97	3.302209	(-0.907836	0.905653	1.287570)
67:	850.36	5.396642	(-2.150190	0.732194	0.487049)
68:	858.61	10.645543	(2.871451	1.210251	-0.967266)
69:	862.43	3.037560	(0.243071	1.323479	1.107646)
70:	866.78	2.450344	(1.239735	0.154848	-0.943093)
71:	873.69	3.417624	(-1.014487	-1.538593	-0.145505)
72:	890.46	20.249416	(4.429072	-0.733654	0.307394)
73:	916.69	0.797799	(-0.524702	-0.719094	-0.073417)
74:	926.04	3.769647	(1.048485	1.600297	0.330719)
75:	933.39	0.747064	(0.370733	-0.372123	-0.686401)
76:	938.28	0.422488	(-0.247076	0.291686	-0.525700)
77:	939.45	1.033376	(-0.990326	0.199208	0.113780)
78:	959.93	14.901576	(-0.329345	-2.386074	-3.016581)
79:	964.64	0.422080	(0.575547	0.299763	0.031112)
80:	966.66	1.082837	(0.850567	-0.534818	0.270818)
81:	971.71	8.223463	(-0.597379	2.784493	0.336449)
82:	972.33	0.877704	(-0.078948	-0.849914	-0.386158)
83:	973.17	6.922752	(0.744441	-2.493357	-0.389526)
84:	985.44	16.996570	(-0.029829	-1.172177	3.952427)
85:	1030.70	30.910893	(3.204148	-3.013751	-3.400240)
86:	1032.35	5.059502	(-1.600147	-1.425538	0.683282)
87:	1036.52	19.666958	(0.931125	2.745388	-3.356011)
88:	1043.52	5.811574	(0.218358	0.976301	-2.193337)
89:	1048.58	15.733908	(2.346897	-2.149363	-2.367746)
90:	1054.81	32.872375	(-5.027804	-0.012316	2.755614)
91:	1073.55	4.060148	(0.323335	-1.467281	-1.342643)
92:	1080.42	6.922347	(0.241324	2.570522	-0.506486)
93:	1090.16	1.136505	(0.514985	0.173346	0.917195)
94:	1108.25	14.278778	(-2.208945	2.927473	-0.910628)
95:	1114.04	19.867474	(-3.585431	0.933564	2.478027)
96:	1115.81	9.878594	(-0.944710	2.997061	0.061180)
97:	1124.94	2.966398	(-0.191633	-1.658869	-0.421696)
98:	1127.34	4.890279	(-0.317125	1.269094	-1.783006)
99:	1129.35	0.503396	(-0.472587	0.081175	-0.522942)
100:	1132.14	1.045092	(-0.046474	-0.777908	-0.661659)
101:	1165.43	1.443316	(0.370308	1.109696	0.273428)
102:	1184.19	17.439872	(0.281697	1.819038	3.748549)
103:	1189.78	15.691152	(-1.557805	-3.549216	0.816983)
104:	1190.70	5.887866	(1.869857	-1.520507	0.282058)
105:	1213.22	5.495933	(-0.836646	-1.182913	1.843007)
106:	1230.59	28.367452	(-1.625858	5.071190	-0.084108)
107:	1236.08	14.284364	(-0.587143	2.690665	2.588426)
108:	1243.19	32.301623	(1.861144	2.659074	4.665521)
109:	1263.90	22.490154	(3.765996	0.784067	2.773566)
110:	1270.81	7.130683	(-1.056664	-2.238869	-1.000805)
111:	1278.43	9.024138	(0.275224	1.360513	2.664093)
112:	1292.42	3.035885	(-0.597062	1.276024	1.025264)
113:	1304.56	6.173137	(1.207118	-0.727461	-2.046168)
114:	1320.45	1.947147	(1.141661	0.662606	0.452451)
115:	1325.27	0.261809	(-0.290583	0.417722	-0.053657)
116:	1329.51	0.044281	(0.033047	0.077885	0.192672)
117:	1348.81	7.593297	(1.425823	1.419877	1.882625)
118:	1356.92	0.992064	(-0.643224	0.758189	0.058962)
119:	1391.35	6.871682	(0.506496	2.218415	-1.301452)
120:	1404.89	30.869923	(-1.261646	-3.854880	-3.797114)
121:	1417.34	17.149193	(-2.911944	1.760340	2.360291)
122:	1421.20	22.028921	(-4.390094	1.191037	1.156472)
123:	1422.54	16.194840	(2.197268	1.211323	-3.146355)
124:	1427.45	9.662446	(2.981779	0.876944	0.049101)
125:	1443.42	83.940519	(3.879705	-7.010318	-4.443405)
126:	1448.55	20.273305	(3.131669	-1.295073	-2.964581)
127:	1451.26	54.167087	(3.182640	3.619575	-5.562065)
128:	1455.74	25.917061	(-1.816808	1.339620	-4.563079)
129:	1527.91	39.997733	(0.512117	3.739899	5.074310)

130:	1535.38	16.208333	(2.136921	-2.253026	2.562377)
131:	1553.72	15.086226)	3.619666	-0.739854	-1.198690)
132:	1561.71	7.570390	(0.226443	1.946385	-1.931502)
133:	1581.71	71.307142)	-1.167333	8.344043	0.566939)
134:	1594.43	25.699635	(-2.134469	0.793711	-4.529205)
135:	1594.92	58.866543)	3.330633	-1.273134	-6.793567)
136:	1597.31	9.621568	(-2.609740	-0.199012	-1.664698)
137:	1643.69	739.806636)	24.571218	7.343257	9.063027)
138:	2901.22	56.191129	(-6.242007	1.157592	-3.986033)
139:	2931.24	32.204301)	-2.958150	-0.867912	-4.764491)
140:	2948.20	41.544660	(5.080426	3.899650	0.725713)
141:	3006.09	2.252007)	0.982304	1.033085	-0.468850)
142:	3014.62	7.055356	(1.339001	-2.292934	-0.069905)
143:	3075.55	10.834761)	-2.838052	-0.558154	-1.571205)
144:	3097.50	10.413059	(-0.218848	1.280847	2.953743)
145:	3102.22	3.971335)	1.017365	0.873028	1.474491)
146:	3105.99	1.257660	(0.697458	0.838344	0.261520)
147:	3107.41	1.491761)	-0.504797	1.110464	0.061738)
148:	3110.35	1.097534	(0.785216	-0.148195	0.677502)
149:	3110.84	5.280229)	-0.793160	0.396837	-2.119822)
150:	3116.21	12.235186	(3.385409	0.879880	-0.000472)
151:	3118.08	0.457051)	-0.304206	0.096995	-0.595905)
152:	3120.60	9.864494	(2.440357	-0.964828	1.725763)
153:	3123.37	22.092084)	3.113215	-1.420598	-3.222092)
154:	3126.32	6.814824	(1.909283	1.625806	0.725408)
155:	3127.76	10.097015)	-2.404281	-0.775050	-1.927627)
156:	3132.33	7.864630	(-1.693785	2.138617	0.649643)
157:	3136.73	11.455401)	0.751800	0.919244	-3.169414)
158:	3138.24	7.099248	(-0.638691	-1.771926	1.884569)

Calculated vibrational frequencies for ${}^1\{3\}\text{-B}$ (${}^1\{\text{FeNO}\}^8$)

Mode	freq (cm**-1)	T**2	TX	TY	TZ
6:	44.43	0.730236	(-0.022712	-0.822914	0.229199)
7:	53.67	0.535117	(0.426617	-0.108024	-0.584334)
8:	56.16	1.327815	(-0.707246	0.832069	0.367804)
9:	69.84	0.728701	(-0.115630	-0.463726	0.707311)
10:	78.93	0.422296	(0.015400	-0.607952	0.229027)
11:	86.55	0.650598	(0.624674	-0.174798	-0.479402)
12:	101.59	0.370942	(-0.062387	-0.602295	0.065502)
13:	120.91	0.299314	(0.042588	-0.448295	0.310695)
14:	123.17	0.509276	(-0.261337	-0.163032	-0.643739)
15:	128.40	1.052137	(-0.487133	-0.394069	0.812126)
16:	140.75	0.419870	(0.155813	0.405077	0.481150)
17:	154.50	2.595769	(-0.709778	-1.179546	0.837052)
18:	165.02	1.577657	(0.131707	0.583998	-1.104199)
19:	201.40	1.915482	(0.342353	-0.497865	-1.245153)
20:	211.72	1.981766	(0.377039	-0.278616	-1.327396)
21:	221.58	0.044279	(0.053250	0.182323	0.090563)
22:	229.77	2.223301	(0.456406	1.416903	0.085916)
23:	249.20	7.059669	(-0.623460	2.441279	-0.843280)
24:	257.31	0.445426	(0.089614	0.648732	-0.128614)
25:	267.93	4.445318	(0.943159	-0.821381	-1.697381)
26:	274.95	2.193485	(-0.275276	1.248370	-0.747851)
27:	285.02	0.675353	(0.208576	-0.789814	0.089678)
28:	306.19	0.146608	(0.189589	-0.212935	0.255583)
29:	322.56	2.383562	(1.300444	0.301207	-0.775681)
30:	331.60	0.206745	(-0.366894	-0.203900	0.174809)
31:	341.86	0.002677	(0.003566	-0.005673	0.051299)
32:	361.27	1.967177	(0.426969	0.423136	-1.267213)
33:	381.82	7.950199	(-2.119715	0.338646	-1.828203)
34:	392.25	10.044561	(-2.421232	-0.469098	-1.990514)
35:	420.38	3.890242	(-0.473714	1.444177	-1.257056)
36:	431.48	0.621248	(-0.026339	-0.439325	0.653872)
37:	440.76	0.504465	(-0.235247	0.665473	-0.079187)
38:	442.95	1.119392	(0.276857	-0.791855	0.644754)
39:	457.94	3.727579	(0.495667	-1.865960	0.009245)
40:	459.55	2.102392	(1.203554	0.170418	-0.790448)
41:	469.16	2.058022	(1.385482	0.170502	-0.330743)
42:	490.67	0.890751	(-0.707841	0.624239	0.006114)
43:	497.77	2.373775	(-0.134822	0.846521	-1.280234)
44:	503.51	6.415272	(0.544152	-2.422755	0.499429)
45:	527.28	1.393811	(-0.928384	-0.725853	-0.071064)
46:	564.41	1.995080	(-1.023006	0.548859	0.804545)
47:	598.27	7.428685	(0.098564	2.075888	-1.763423)
48:	615.22	8.818898	(-0.378400	-2.507634	1.545148)
49:	625.63	6.041916	(-1.255320	0.649147	2.011143)
50:	634.96	3.174003	(1.207476	-0.079767	1.307533)
51:	642.36	3.995644	(0.598837	-1.730409	-0.801700)
52:	652.27	7.821507	(0.724187	1.296660	-2.369754)
53:	664.97	4.039725	(-0.368395	1.712534	-0.985513)
54:	680.25	9.829811	(-2.712255	0.451292	1.506593)
55:	686.84	0.414503	(-0.625773	-0.059199	-0.139308)
56:	722.03	3.921706	(-0.753176	1.810111	0.279162)
57:	733.28	31.030976	(2.424246	-5.015319	0.024047)
58:	736.53	12.001528	(0.546391	-2.858223	1.879773)
59:	738.64	14.594434	(0.146027	-3.481259	1.566508)
60:	741.68	24.482886	(-1.128930	-4.476795	1.779525)
61:	743.97	42.079826	(-4.837871	2.982705	3.127027)
62:	745.89	9.291183	(-1.675774	-0.235396	2.535262)
63:	773.40	3.497016	(-1.037195	0.678140	1.400489)
64:	818.06	5.884448	(0.949416	-1.897226	1.176261)

65:	827.21	4.473177	(0.097426	-0.657640	-2.007784)
66:	848.26	4.352520	(0.926997	-0.398908	1.825943)
67:	851.43	12.608710	(3.441060	-0.040809	-0.875301)
68:	856.95	10.862081	(2.543132	1.148724	-1.753566)
69:	862.44	3.665153	(-1.585566	-0.250446	-1.043269)
70:	870.87	6.275747	(2.448973	0.526888	-0.025868)
71:	876.31	19.209659	(3.635789	-1.947038	1.483152)
72:	877.06	2.052958	(-0.155751	-1.215372	-0.742677)
73:	913.39	4.076264	(-0.863989	1.286840	1.293765)
74:	923.64	2.257465	(-0.113579	-1.072033	-1.046571)
75:	936.41	1.274069	(-0.273416	-1.091335	-0.091103)
76:	939.52	0.167214	(-0.302472	-0.084277	0.261959)
77:	942.19	5.573833	(-1.330717	-0.208071	1.939003)
78:	951.05	11.906156	(-0.782992	0.792866	3.265646)
79:	966.50	0.279980	(0.356621	0.352885	0.168146)
80:	973.89	0.165679	(-0.278171	0.136833	-0.263773)
81:	974.39	0.735817	(0.222971	0.332306	-0.758732)
82:	978.37	0.654953	(0.533360	0.581403	-0.180141)
83:	991.09	12.917632	(0.606507	-3.394715	-1.012763)
84:	995.59	30.630721	(0.256498	-3.939969	3.878347)
85:	1011.03	8.908403	(0.931363	1.291586	2.524435)
86:	1031.81	20.281406	(-2.328443	3.209037	2.135846)
87:	1033.54	9.824346	(-2.456616	-0.736039	1.802118)
88:	1037.30	18.575569	(0.974226	2.360461	-3.471985)
89:	1045.02	7.040734	(-0.045374	1.005803	-2.455002)
90:	1052.15	23.527015	(-4.217182	0.278224	2.380123)
91:	1059.49	2.867796	(-1.547224	0.562091	0.397425)
92:	1077.90	5.393698	(0.325557	-1.970513	1.185238)
93:	1089.61	1.585061	(-0.881034	-0.653501	-0.617882)
94:	1091.79	5.209564	(2.055191	0.711912	0.692053)
95:	1113.04	5.452613	(1.570226	0.101477	-1.725313)
96:	1120.91	10.508521	(0.467893	-2.923345	1.320473)
97:	1123.98	0.753043	(0.614846	-0.521592	0.320855)
98:	1126.38	0.546419	(-0.119427	-0.639007	0.351890)
99:	1129.13	2.088777	(1.445014	0.023985	0.011710)
100:	1132.62	0.980018	(-0.071512	-0.877106	-0.453418)
101:	1166.99	0.835133	(0.303993	0.834084	0.216853)
102:	1180.20	10.725751	(0.615792	1.349092	2.920017)
103:	1189.28	4.680408	(-1.944801	-0.582040	-0.747922)
104:	1192.32	11.264467	(-0.468406	-3.239853	0.740551)
105:	1208.62	2.373164	(0.633117	1.029677	-0.955036)
106:	1229.05	9.451771	(-0.905749	2.915132	-0.365232)
107:	1235.09	16.830216	(-2.305232	-1.054893	-3.225418)
108:	1240.99	9.610409	(2.403249	0.611281	1.860414)
109:	1259.30	24.968327	(3.950095	0.736745	2.970232)
110:	1266.12	2.097990	(-0.942820	-0.979056	0.500529)
111:	1273.49	11.692442	(1.207325	1.278899	2.932444)
112:	1279.57	3.576104	(0.184890	0.975987	1.609152)
113:	1295.62	0.841075	(0.050698	0.427311	0.809883)
114:	1315.54	2.365886	(1.072649	-0.033335	1.101907)
115:	1324.45	1.122767	(-0.129706	-0.922037	0.505758)
116:	1329.57	1.182670	(0.120170	1.035063	0.311247)
117:	1346.10	3.865548	(-0.161276	-0.933276	-1.722943)
118:	1356.07	1.951344	(0.634041	-1.111732	-0.559811)
119:	1396.47	13.197026	(-1.386838	-3.282741	0.705209)
120:	1407.30	24.844618	(-0.764673	-2.892491	-3.986652)
121:	1416.27	16.229281	(1.770711	-3.263786	-1.562551)
122:	1419.35	31.792560	(1.303598	3.434736	-4.277357)
123:	1422.02	32.906015	(-5.144264	-0.674123	2.447063)
124:	1423.98	5.848787	(-2.373036	-0.373577	0.279155)
125:	1449.12	20.247594	(-2.900877	0.832159	3.337666)
126:	1450.94	29.667265	(-0.604377	5.258525	-1.284486)
127:	1453.26	28.469292	(-2.402452	-1.055912	4.645704)
128:	1457.20	37.994596	(5.842258	1.050202	1.661232)

129:	1490.36	510.980517	(19.885503	7.891896	7.298305)
130:	1533.95	1.503404)	-0.372759	-0.844954	0.806541)
131:	1535.76	2.896973	(-1.699490	-0.008899	0.092892)
132:	1557.00	6.609801)	-2.444905	0.662286	0.440019)
133:	1562.39	9.979390	(2.908327	0.393087	-1.168977)
134:	1591.99	36.569121)	1.913023	-5.674569	0.841863)
135:	1596.02	23.467559	(-3.718301	1.068414	2.915525)
136:	1599.01	22.182779)	2.542257	0.654607	-3.910396)
137:	1606.89	25.816817	(2.664027	2.551332	-3.494350)
138:	2899.73	66.512157)	-6.857489	1.557143	-4.130655)
139:	2935.81	40.183567	(-2.829038	-1.246505	-5.534107)
140:	2952.45	36.120919)	4.951179	3.333098	0.705129)
141:	3005.80	2.396586	(0.714206	1.349892	-0.253552)
142:	3015.10	4.451700)	-1.649884	1.216132	0.500607)
143:	3076.74	10.832253	(-2.733724	-0.624096	-1.723226)
144:	3098.47	8.706980)	0.040410	-1.158053	-2.713717)
145:	3104.77	1.524584	(0.783294	-0.927169	0.226698)
146:	3106.64	1.433964)	-0.173156	0.515880	-1.066700)
147:	3110.70	1.265135	(-0.333458	-0.319147	1.025712)
148:	3112.33	0.911940)	0.146367	0.821040	0.465198)
149:	3113.41	5.672556	(-1.130466	-0.124704	-2.092618)
150:	3115.83	10.720359)	-3.110527	-0.980523	-0.289058)
151:	3119.23	0.361513	(-0.179470	0.016339	0.573617)
152:	3123.25	23.122964)	3.309465	-1.375286	-3.206087)
153:	3124.63	5.362557	(-1.815605	0.855258	-1.155279)
154:	3126.09	4.897724)	1.587287	1.226983	0.934215)
155:	3129.42	8.554868	(1.663629	0.415042	2.369588)
156:	3136.22	8.464673)	-1.210576	2.417343	1.075004)
157:	3137.46	21.585273	(-1.355683	-2.236258	3.840123)
158:	3137.51	0.484530)	0.081744	-0.691218	0.008097)

Calculated vibrational frequencies for ${}^4\{1\}$ (${}^4\{\text{FeNO}\}^7$)

Mode	freq (cm**-1)	T**2	TX	TY	TZ
6:	39.73	1.011589	(0.141237	-0.994949	0.041428)
7:	47.16	0.287487	(-0.307410	-0.038593	0.437604)
8:	50.59	0.952662	(0.777062	-0.209805	-0.552104)
9:	57.79	0.190665	(0.156767	0.407485	0.006709)
10:	63.86	0.795153	(0.021004	0.753869	-0.475807)
11:	69.04	1.532273	(0.471022	-0.545331	1.006492)
12:	84.10	0.541441	(0.320104	0.654831	-0.100850)
13:	90.42	0.149775	(0.373531	-0.005939	-0.101063)
14:	99.21	0.305988	(0.413354	-0.206634	0.304021)
15:	103.14	1.137132	(0.163020	0.848058	-0.625583)
16:	107.80	0.204968	(-0.028585	-0.249131	0.376940)
17:	127.71	0.204339	(0.220718	0.111252	0.378478)
18:	143.19	0.871057	(-0.201988	0.597518	-0.687917)
19:	165.89	2.829183	(-0.370373	-1.636599	0.116402)
20:	179.17	0.421005	(-0.632308	-0.117921	0.085358)
21:	185.12	5.239093	(0.142577	1.270921	-1.898295)
22:	198.77	0.449323	(0.085101	-0.103667	-0.656760)
23:	218.92	2.080428	(-0.478108	1.182496	-0.673456)
24:	227.28	4.699692	(0.065548	0.934551	-1.954996)
25:	240.39	4.709487	(-1.043283	1.565812	1.081332)
26:	260.07	1.300821	(0.341198	1.088270	-0.008530)
27:	268.66	0.716036	(0.754109	-0.330346	0.195518)
28:	275.16	2.671493	(-0.695717	-0.133625	-1.472961)
29:	296.80	15.058406	(1.898092	-2.639325	-2.118871)
30:	307.93	3.940020	(-0.162965	-0.852243	1.785258)
31:	319.49	4.930162	(0.996056	-1.309320	-1.491213)
32:	341.03	3.086362	(-1.000774	0.896958	1.131494)
33:	389.13	4.097562	(0.124239	1.557768	1.286656)
34:	394.55	6.748944	(-2.581838	-0.276375	0.081682)
35:	410.09	1.614991	(0.180404	-1.256111	0.068044)
36:	417.57	6.310514	(-1.532639	1.955768	-0.369465)
37:	423.97	2.120736	(-0.515489	0.286365	1.331541)
38:	430.03	1.793550	(1.012241	0.837719	-0.259125)
39:	434.66	3.354243	(-1.404304	0.913945	0.739512)
40:	445.44	3.852512	(-0.503170	1.800407	-0.598219)
41:	455.86	2.483412	(-1.255651	-0.863547	0.401297)
42:	474.32	0.221383	(0.185949	0.358145	-0.241945)
43:	476.07	1.910763	(1.294640	-0.227133	0.427880)
44:	482.19	3.571131	(0.213152	1.673207	-0.852100)
45:	522.62	2.917341	(0.526074	1.543428	-0.508347)
46:	559.94	6.121006	(1.719126	-0.661751	-1.651574)
47:	585.51	2.736127	(-0.930960	-1.083104	-0.834462)
48:	598.63	1.723357	(0.741398	-0.856733	-0.663094)
49:	617.73	4.154424	(0.467763	-1.982115	-0.082719)
50:	627.15	2.634184	(0.815470	-0.078749	-1.401068)
51:	631.65	1.047346	(-0.109844	-0.679304	0.757513)
52:	642.02	0.455241	(-0.285005	0.550153	-0.267104)
53:	647.30	1.882478	(-0.981541	-0.933984	0.216168)
54:	680.39	8.709148	(2.424997	-0.754736	-1.502967)
55:	689.12	1.185175	(-0.762803	-0.212743	-0.747025)
56:	727.96	1.796191	(-0.290614	1.220605	-0.471018)
57:	737.65	5.148029	(1.086748	-1.976857	0.242989)
58:	744.64	6.872385	(0.731472	-2.458155	-0.542960)
59:	745.95	27.099190	(-0.241555	5.081679	-1.103347)
60:	747.99	37.755337	(2.118694	-5.642950	1.193142)
61:	751.88	29.932491	(4.577583	-1.025777	-2.815316)
62:	760.50	14.050303	(-0.342665	3.637033	-0.839567)
63:	787.89	7.802651	(-1.814993	-0.091129	2.121355)
64:	826.74	1.462973	(0.748694	-0.052784	-0.948496)

65:	830.54	3.549555	(-1.680797	0.662183	0.534780)
66:	859.24	11.158717	(-3.331352	-0.185221	-0.162802)
67:	862.18	2.085521	(-1.085980	0.008879	0.951887)
68:	870.42	7.475870	(-2.685449	0.453964	0.241146)
69:	875.91	2.511432	(-0.681458	1.358346	-0.449382)
70:	885.91	8.063767	(-2.765812	0.481131	-0.427273)
71:	890.87	1.793130	(-0.635674	-1.128353	-0.340395)
72:	895.18	2.438033	(0.904289	-0.463163	-1.185653)
73:	918.80	5.157033	(-0.700924	-1.900627	-1.026332)
74:	941.35	2.861164	(-0.301155	-1.440976	-0.833102)
75:	953.63	0.671606	(-0.599394	0.073440	-0.554021)
76:	962.39	9.939540	(0.300597	1.343826	2.836074)
77:	963.53	1.081176	(0.125084	0.008135	1.032213)
78:	966.41	4.888534	(0.008542	0.943056	1.999777)
79:	982.84	0.192677	(-0.204903	-0.248699	-0.298062)
80:	989.61	9.123608	(-0.829028	2.740361	0.962675)
81:	992.96	13.267857	(-1.141002	-1.038988	3.299466)
82:	993.87	0.939134	(-0.146704	0.081257	0.954468)
83:	997.04	1.791652	(0.644848	-0.221514	-1.151848)
84:	1002.45	0.029156	(0.072499	-0.056081	-0.144064)
85:	1002.77	0.195773	(0.413237	-0.117152	-0.106225)
86:	1036.60	7.875223	(2.079508	-0.277793	-1.863787)
87:	1041.47	2.091691	(-0.434546	1.033884	0.913206)
88:	1045.48	4.031404	(0.833297	0.935745	-1.568886)
89:	1047.42	1.140611	(-0.296125	0.401420	-0.944343)
90:	1048.43	4.555008	(-1.943816	-0.609298	0.636666)
91:	1057.17	7.903693	(1.860074	-1.233054	-1.709794)
92:	1081.95	7.566680	(-0.295787	-0.423175	2.701872)
93:	1093.08	6.938607	(0.500567	1.661678	-1.981632)
94:	1095.82	6.182976	(2.071918	-0.231698	1.355155)
95:	1103.24	5.541341	(0.274566	2.040893	-1.140487)
96:	1116.54	1.186490	(-0.292773	0.146823	1.038854)
97:	1137.18	1.630870	(-0.815957	0.668658	-0.719709)
98:	1137.63	2.734019	(1.042933	-0.023716	1.282867)
99:	1138.64	1.790825	(-0.966839	-0.848913	-0.367960)
100:	1141.74	0.482489	(-0.141814	-0.631323	-0.252604)
101:	1170.56	0.503740	(-0.473993	-0.520991	-0.087401)
102:	1188.33	3.044832	(1.003845	1.384512	0.346777)
103:	1192.93	2.816895	(-0.096440	-1.671674	-0.114452)
104:	1196.72	8.244647	(0.311236	-1.430598	-2.470054)
105:	1215.59	2.325560	(-0.681361	-1.313624	-0.368373)
106:	1240.69	1.516620	(0.086571	-0.310122	1.188675)
107:	1247.64	11.361229	(0.262674	1.869492	-2.792352)
108:	1254.75	14.401564	(2.964528	-0.702380	-2.262697)
109:	1270.51	17.564285	(-4.115842	0.598110	0.516131)
110:	1276.65	4.993716	(-0.838807	-1.394150	-1.531818)
111:	1283.84	3.460733	(-0.164143	-1.695509	0.747689)
112:	1288.12	8.890750	(1.438560	1.008334	2.409265)
113:	1303.13	1.095716	(-0.680433	0.769370	-0.201983)
114:	1327.41	1.732126	(0.555893	-0.130270	-1.185807)
115:	1332.10	0.040960	(0.004920	-0.198792	-0.037654)
116:	1335.38	0.128901	(0.133768	0.243645	-0.227254)
117:	1353.75	3.163651	(0.355126	-0.026670	1.742649)
118:	1358.83	2.383774	(1.455574	0.344798	-0.382352)
119:	1401.24	7.705510	(-1.217040	-2.480936	0.263207)
120:	1411.06	14.196261	(2.189452	0.828621	2.952278)
121:	1425.08	10.100079	(-3.132263	-0.535269	0.049951)
122:	1426.94	3.042644	(1.034843	1.283743	-0.568987)
123:	1428.66	11.937911	(-2.660993	1.624905	-1.488862)
124:	1431.85	11.791219	(1.872125	2.120028	1.947266)
125:	1450.68	40.112458	(-1.647623	5.945605	-1.430938)
126:	1453.10	27.983148	(-3.271180	-0.280020	4.147785)
127:	1462.17	10.794459	(0.841157	1.051866	-2.996747)
128:	1463.36	26.671167	(4.638948	0.918122	2.075664)

129:	1567.50	3.330219	(-1.811252	0.044242	0.218237)
130:	1571.58	2.619027	(0.857441	-0.850944	1.076901)
131:	1573.84	7.126949	(-0.972769	2.436708	-0.493076)
132:	1576.72	0.202641	(-0.164614	0.390131	-0.152777)
133:	1595.48	7.240478	(-1.304717	0.751111	2.230252)
134:	1600.81	29.340575	(1.171639	-5.185198	-1.039982)
135:	1606.51	29.712780	(-0.664013	-0.755898	5.357283)
136:	1607.04	7.022722	(1.917983	0.546556	-1.745090)
137:	1724.50	842.051284	(28.636657	4.558110	1.103073)
138:	2940.64	32.295635	(4.255176	-0.995190	3.633002)
139:	2961.46	19.334415	(-1.730860	-1.144840	-3.876581)
140:	2975.38	16.259985	(2.915953	2.697984	0.691439)
141:	3029.06	2.137861	(1.385720	-0.455695	0.099921)
142:	3034.67	3.984170	(-0.975439	-1.564672	0.764519)
143:	3092.33	4.700801	(-1.702787	-0.390018	-1.284214)
144:	3113.20	4.327463	(-1.418830	1.518086	-0.098987)
145:	3115.39	2.976341	(0.804396	0.996116	-1.156304)
146:	3115.71	1.473829	(-0.024992	0.422964	1.137676)
147:	3118.47	0.155134	(-0.036875	0.268085	0.286189)
148:	3122.73	1.754211	(-0.535818	0.465160	-1.118363)
149:	3125.28	0.348525	(0.085305	0.367942	0.453725)
150:	3126.99	1.192709	(-0.778283	-0.514052	-0.568098)
151:	3129.36	0.177842	(0.173267	-0.370794	0.101648)
152:	3131.41	0.267517	(0.382650	0.020779	0.347367)
153:	3135.66	5.649651	(-1.897092	0.562926	1.316742)
154:	3137.14	0.098143	(0.279512	0.059917	0.128164)
155:	3138.66	0.838696	(0.694480	0.035695	0.595919)
156:	3143.61	0.251956	(-0.344572	0.345572	0.117498)
157:	3146.81	0.440042	(0.167209	-0.464433	0.443153)
158:	3148.26	0.079388	(-0.131910	0.078892	0.236144)

Calculated vibrational frequencies for ${}^2\{1\}$ (${}^2\{\text{FeNO}\}^7$)

Mode	freq (cm**-1)	T**2	TX	TY	TZ
6:	46.97	1.379134	(0.019303	1.123190	-0.342352)
7:	55.28	0.641523	(-0.575744	0.173814	0.528990)
8:	57.38	0.997106	(0.623543	-0.739329	-0.248380)
9:	64.96	0.258560	(-0.389435	0.315834	-0.084550)
10:	76.16	0.569786	(0.017364	0.459816	-0.598376)
11:	86.80	0.315048	(0.405471	-0.212781	0.324601)
12:	101.65	0.373890	(-0.134328	-0.290935	0.520771)
13:	119.86	0.125859	(-0.120729	-0.332283	-0.029509)
14:	122.36	0.436742	(-0.400085	-0.140011	-0.507022)
15:	127.91	0.399899	(-0.465014	-0.080075	0.421009)
16:	133.76	1.867538	(0.458112	0.801645	-1.007491)
17:	139.19	0.535333	(-0.213660	0.302833	0.630852)
18:	156.88	0.248906	(-0.492505	0.054092	0.058472)
19:	207.07	0.139421	(0.018286	-0.011704	0.372759)
20:	222.68	0.728125	(0.207001	0.820763	-0.107816)
21:	224.87	1.555714	(-0.023513	1.142060	0.500860)
22:	244.51	3.116591	(-0.425634	1.707833	-0.136875)
23:	248.43	0.620275	(-0.739363	-0.170764	0.210847)
24:	260.73	0.600909	(-0.331037	0.243083	0.657446)
25:	272.47	2.382920	(-0.575221	1.424180	0.154117)
26:	284.02	0.601256	(0.657750	-0.102554	-0.397623)
27:	291.89	0.611759	(0.736185	-0.216986	-0.150689)
28:	304.01	0.473682	(-0.202577	-0.623535	-0.209399)
29:	321.93	0.500455	(-0.363547	0.251964	0.552089)
30:	333.22	0.649583	(-0.279103	0.668262	-0.353708)
31:	345.39	0.575133	(0.311072	-0.047588	-0.690002)
32:	361.45	0.142001	(-0.194707	0.088227	0.310333)
33:	387.90	0.071692	(-0.032529	0.180571	0.195007)
34:	414.63	4.880125	(-1.509488	-1.408546	-0.785855)
35:	429.23	3.504112	(1.491786	-0.140786	1.121992)
36:	430.62	1.111137	(0.344846	0.979011	-0.183726)
37:	440.17	0.225990	(0.217789	0.074867	0.415876)
38:	451.50	0.417493	(-0.579385	-0.214501	-0.189197)
39:	456.78	4.127731	(-1.820201	0.871492	0.234733)
40:	461.13	3.128188	(-0.734565	-1.482619	0.624855)
41:	481.29	1.372428	(-0.268120	-0.963007	0.610867)
42:	485.63	0.594107	(-0.753192	0.163337	0.011384)
43:	493.63	2.432530	(-0.662360	1.411779	0.026266)
44:	516.00	4.414153	(0.337631	1.876874	-0.881760)
45:	526.76	2.031338	(1.205239	0.668104	-0.363835)
46:	562.10	3.957024	(1.462544	-0.446456	-1.272268)
47:	599.81	1.634911	(-0.257129	1.144253	-0.509393)
48:	622.11	0.334359	(0.571477	0.063596	0.061064)
49:	628.02	1.259477	(1.068246	-0.315709	-0.136584)
50:	637.74	0.395091	(-0.509395	-0.342545	-0.135169)
51:	644.34	1.920725	(0.290526	-1.275308	-0.458158)
52:	652.03	1.931119	(0.518213	0.640498	-1.119078)
53:	659.13	4.226242	(0.045346	-1.104146	1.733507)
54:	684.02	6.892615	(2.142447	-0.758205	-1.314405)
55:	691.37	0.905668	(0.950865	0.004705	0.038737)
56:	721.55	3.097018	(-0.827722	1.533476	0.245651)
57:	738.94	2.478971	(-0.639664	1.413500	-0.267989)
58:	745.16	24.568012	(-1.616229	4.676725	-0.289924)
59:	747.45	35.977918	(1.938448	-5.481174	1.475490)
60:	750.51	6.378116	(-0.531900	-2.441162	0.368683)
61:	755.10	23.148680	(0.681772	4.347742	-1.944481)
62:	756.34	42.655420	(5.070311	-2.081605	-3.551660)
63:	782.62	5.951047	(1.454151	-0.322322	-1.931994)
64:	823.04	1.943732	(1.088511	-0.363981	-0.791450)

65:	831.43	1.043678	(0.931459	-0.007293	0.419534)
66:	852.61	10.402671	(3.216634	-0.228789	-0.059909)
67:	859.28	6.490207	(-2.541136	0.030064	0.178692)
68:	865.35	4.095427	(1.833518	-0.131682	-0.846343)
69:	869.12	0.716952	(0.445984	-0.532123	0.484659)
70:	882.34	10.082682	(3.144238	-0.443066	-0.011969)
71:	885.65	1.520455	(1.186205	0.174988	0.287667)
72:	890.92	0.593128	(0.679123	-0.256992	-0.256662)
73:	911.79	4.531500	(-0.135221	-1.687731	-1.290264)
74:	938.96	2.358040	(-0.230610	-1.135073	-1.008200)
75:	949.39	0.689847	(-0.647281	0.428235	-0.295786)
76:	955.29	7.346039	(0.122292	-0.872183	-2.563275)
77:	957.63	0.570619	(-0.047001	-0.577307	0.484898)
78:	960.28	1.039054	(0.111930	0.330442	0.957775)
79:	982.60	0.208741	(0.284448	0.281207	0.220799)
80:	991.67	0.236409	(-0.164648	-0.409773	0.203435)
81:	996.29	0.041742	(0.139485	0.146889	0.026639)
82:	996.85	0.220644	(0.403477	0.190726	-0.146541)
83:	998.91	0.909761	(0.318436	0.833927	-0.336044)
84:	1006.55	0.313007	(0.288089	-0.317725	0.359253)
85:	1012.46	1.954108	(0.856468	0.408610	1.026454)
86:	1033.49	5.976828	(1.897151	-0.346910	-1.502431)
87:	1039.89	2.512625	(0.844371	-1.233848	-0.526575)
88:	1045.22	0.235891	(-0.241455	0.125756	0.402214)
89:	1047.16	4.726195	(1.031314	1.302533	-1.402139)
90:	1050.16	2.594133	(-0.458149	0.680501	-1.386056)
91:	1052.60	9.823700	(-2.726297	0.258377	1.524548)
92:	1081.49	7.832352	(-0.195386	2.009637	-1.937920)
93:	1095.12	2.269843	(0.278689	1.292909	-0.721500)
94:	1099.81	5.418932	(2.064245	0.245077	1.047740)
95:	1102.94	4.054385	(-0.646752	-1.906839	0.007898)
96:	1116.80	1.811301	(0.330589	-0.427404	-1.232614)
97:	1136.33	0.863998	(0.698194	-0.468883	0.395818)
98:	1138.18	1.392446	(1.013644	0.248297	0.550746)
99:	1139.55	0.693353	(-0.657092	-0.441457	-0.258260)
100:	1140.56	0.776912	(-0.241000	-0.757362	-0.381096)
101:	1169.31	2.151132	(-0.163239	-1.454750	-0.090479)
102:	1184.47	3.252084	(1.236275	0.896482	0.959181)
103:	1193.25	2.892897	(-0.365115	-1.638124	-0.275929)
104:	1196.19	6.476368	(-0.805944	-1.409957	-1.959297)
105:	1214.79	1.878049	(-0.544131	-0.804298	0.966993)
106:	1235.29	0.833193	(-0.196899	-0.810150	0.371591)
107:	1242.98	3.843044	(0.451900	1.155198	-1.518008)
108:	1247.69	9.475778	(3.065197	0.269045	0.089224)
109:	1266.60	10.991307	(-2.904041	-0.192842	-1.587660)
110:	1270.63	4.022897	(1.581675	0.562046	1.097865)
111:	1281.16	0.510232	(0.671319	0.124728	-0.209777)
112:	1282.21	13.671104	(1.610222	1.035812	3.163129)
113:	1298.89	0.213927	(-0.139449	0.436084	-0.065661)
114:	1320.07	0.174939	(0.391461	-0.069651	0.129791)
115:	1329.28	0.440407	(0.118117	0.055212	-0.650697)
116:	1332.61	0.667655	(0.002159	-0.804179	-0.144731)
117:	1348.11	3.565950	(-0.006264	-0.020849	1.888247)
118:	1359.56	1.655887	(0.994532	0.773732	-0.261020)
119:	1395.29	9.121084	(0.496741	2.533681	-1.566779)
120:	1409.12	22.132295	(2.075825	2.462292	3.429338)
121:	1426.77	8.874833	(1.040595	-0.655503	-2.713358)
122:	1427.11	12.641352	(3.413080	-0.694817	-0.713769)
123:	1429.48	15.095218	(-3.164594	-2.154253	0.663143)
124:	1432.98	10.112337	(-0.997988	0.066981	-3.018588)
125:	1451.87	20.315029	(-2.932205	0.652639	3.360247)
126:	1454.20	37.611125	(-1.249928	5.776999	-1.635571)
127:	1461.98	21.347450	(-2.858094	-1.202645	3.425258)
128:	1465.52	27.338719	(4.519343	1.054815	2.408657)

129:	1561.34	1.127802	(0.151212	0.899726	0.543536)
130:	1563.48	3.321270)	-1.526232	-0.790613	-0.605653)
131:	1567.03	2.241691	(1.471136	-0.245333	0.131387)
132:	1570.13	0.476187)	0.480241	-0.436511	-0.234549)
133:	1596.66	13.657459	(-2.023556	1.094720	2.892104)
134:	1603.69	0.152294)	-0.387690	0.036200	0.026075)
135:	1610.11	5.277665	(0.388629	0.895128	-2.079754)
136:	1613.40	0.088963)	-0.219380	-0.151415	0.133823)
137:	1681.31	602.542957	(23.186053	6.370197	4.936646)
138:	2947.05	28.457583)	3.992411	-0.828619	3.439713)
139:	2983.04	6.076896	(-1.394287	-1.750846	1.033149)
140:	2986.15	20.528346)	2.581753	1.807768	3.254976)
141:	3024.36	2.843587	(1.258134	1.023761	-0.461087)
142:	3034.01	2.067726)	-1.406867	0.284338	0.087199)
143:	3090.73	4.975642	(1.771238	0.489959	1.264238)
144:	3114.90	1.925570)	0.047614	-0.544344	-1.275536)
145:	3125.10	0.107646	(0.195522	-0.048072	0.259048)
146:	3127.32	1.666441)	1.054509	0.542998	0.509514)
147:	3128.42	0.169882	(0.212983	0.291109	-0.199440)
148:	3130.89	0.278392)	0.086138	-0.232955	0.465515)
149:	3131.81	1.107981	(0.420998	-0.947827	-0.179906)
150:	3134.70	1.635249)	-0.180717	0.326113	-1.223209)
151:	3135.15	6.143722	(1.865181	-0.605478	-1.515987)
152:	3138.59	0.771883)	0.390807	-0.699666	-0.360028)
153:	3138.91	0.235872	(-0.192562	-0.415286	0.162264)
154:	3141.02	0.612336)	-0.054704	-0.226178	0.747120)
155:	3144.94	0.542736	(0.037810	-0.183385	0.712514)
156:	3148.42	0.060473)	-0.078865	0.230735	0.031854)
157:	3151.29	0.210118	(-0.192438	-0.376165	-0.177722)
158:	3151.39	0.364204)	0.027273	0.430891	-0.421655)

Coordinates for Initial Guess A (IGA) (\angle [Fe-N-O] = 179.8°)

Fe	10.1561280000	2.3633820000	3.6201180000
S	9.4498810000	4.3527100000	4.5236180000
C	7.7609210000	4.1235350000	4.9744970000
C	7.3164570000	4.6276900000	6.2012090000
H	7.9385890000	5.0225260000	6.8016520000
C	5.9789900000	4.5570060000	6.5492920000
H	5.6877300000	4.9156950000	7.3799180000
C	5.0679280000	3.9675320000	5.6978920000
H	4.1487110000	3.9322630000	5.9370590000
C	5.4956150000	3.4276690000	4.4939180000
H	4.8698710000	3.0000520000	3.9215470000
C	6.8369270000	3.5069880000	4.1174840000
C	7.2593700000	3.0240520000	2.7624870000
H	6.4566570000	2.7263890000	2.2653460000
H	7.6601450000	3.7800660000	2.2653460000
C	8.7047200000	1.5736370000	1.4282630000
H	7.9479100000	1.3229500000	0.8252930000
C	9.4406770000	2.8040970000	0.9454380000
C	9.2579980000	3.4067420000	-0.2868880000
H	8.6457690000	3.0468820000	-0.9179280000
C	9.9867310000	4.5431030000	-0.5771440000
H	9.8783830000	4.9830130000	-1.4119810000
C	10.8768230000	5.0354040000	0.3638030000
H	11.3882760000	5.8127840000	0.1740410000
C	11.0174430000	4.3909050000	1.5750750000
H	11.6259440000	4.7342280000	2.2176250000
C	9.7285580000	0.4763500000	1.5436350000
C	9.8803630000	-0.5580100000	0.6428300000
H	9.2935320000	-0.6512310000	-0.0982490000
C	10.9166670000	-1.4570010000	0.8536450000
H	11.0504140000	-2.1805260000	0.2526410000
C	11.7501380000	-1.2951440000	1.9374740000
H	12.4566180000	-1.9097890000	2.0969190000
C	11.5421780000	-0.2193700000	2.7925230000
H	12.1210870000	-0.1024410000	3.5369710000
C	7.6932320000	0.7456230000	3.5619550000
H	7.9875210000	-0.0995140000	3.1383600000
H	6.7036460000	0.7726960000	3.5453930000
C	8.1770730000	0.7968430000	4.9809540000
C	7.4539320000	0.2413210000	6.0237990000
H	6.6011220000	-0.1478070000	5.8668810000
C	7.9898510000	0.2602000000	7.2965470000
H	7.5086890000	-0.1141480000	8.0255560000
C	9.2282900000	0.8265510000	7.4997830000
H	9.6139180000	0.8414780000	8.3680250000
C	9.9005180000	1.3725600000	6.4257780000
H	10.7533280000	1.7663720000	6.5686610000
N	8.2411510000	1.9026180000	2.8090850000
N	10.3070010000	3.2845450000	1.8616820000
N	10.5509610000	0.6544500000	2.5985510000
N	9.3851040000	1.3639260000	5.1822240000
N	11.7721570000	2.6314110000	4.1845740000
O	12.8449533439	2.8113722896	4.5566950348

Coordinates for Initial Guess B (IGB) (\angle [Fe-N-O] = 147.2°)

Fe	10.1561280000	2.3633820000	3.6201180000
S	9.4498810000	4.3527100000	4.5236180000
C	7.7609210000	4.1235350000	4.9744970000
C	7.3164570000	4.6276900000	6.2012090000
H	7.9385890000	5.0225260000	6.8016520000
C	5.9789900000	4.5570060000	6.5492920000
H	5.6877300000	4.9156950000	7.3799180000
C	5.0679280000	3.9675320000	5.6978920000
H	4.1487110000	3.9322630000	5.9370590000
C	5.4956150000	3.4276690000	4.4939180000
H	4.8698710000	3.0000520000	3.9215470000
C	6.8369270000	3.5069880000	4.1174840000
C	7.2593700000	3.0240520000	2.7624870000
H	6.4566570000	2.7263890000	2.2653460000
H	7.6601450000	3.7800660000	2.2653460000
C	8.7047200000	1.5736370000	1.4282630000
H	7.9479100000	1.3229500000	0.8252930000
C	9.4406770000	2.8040970000	0.9454380000
C	9.2579980000	3.4067420000	-0.2868880000
H	8.6457690000	3.0468820000	-0.9179280000
C	9.9867310000	4.5431030000	-0.5771440000
H	9.8783830000	4.9830130000	-1.4119810000
C	10.8768230000	5.0354040000	0.3638030000
H	11.3882760000	5.8127840000	0.1740410000
C	11.0174430000	4.3909050000	1.5750750000
H	11.6259440000	4.7342280000	2.2176250000
C	9.7285580000	0.4763500000	1.5436350000
C	9.8803630000	-0.5580100000	0.6428300000
H	9.2935320000	-0.6512310000	-0.0982490000
C	10.9166670000	-1.4570010000	0.8536450000
H	11.0504140000	-2.1805260000	0.2526410000
C	11.7501380000	-1.2951440000	1.9374740000
H	12.4566180000	-1.9097890000	2.0969190000
C	11.5421780000	-0.2193700000	2.7925230000
H	12.1210870000	-0.1024410000	3.5369710000
C	7.6932320000	0.7456230000	3.5619550000
H	7.9875210000	-0.0995140000	3.1383600000
H	6.7036460000	0.7726960000	3.5453930000
C	8.1770730000	0.7968430000	4.9809540000
C	7.4539320000	0.2413210000	6.0237990000
H	6.6011220000	-0.1478070000	5.8668810000
C	7.9898510000	0.2602000000	7.2965470000
H	7.5086890000	-0.1141480000	8.0255560000
C	9.2282900000	0.8265510000	7.4997830000
H	9.6139180000	0.8414780000	8.3680250000
C	9.9005180000	1.3725600000	6.4257780000
H	10.7533280000	1.7663720000	6.5686610000
N	8.2411510000	1.9026180000	2.8090850000
N	10.3070010000	3.2845450000	1.8616820000
N	10.5509610000	0.6544500000	2.5985510000
N	9.3851040000	1.3639260000	5.1822240000
N	11.7721570000	2.6314110000	4.1845740000
O	12.7082670000	3.2994720000	4.1550990000

Coordinates for Initial Guess C (IGC) (\angle [Fe-N-O] = 119.7°)

Fe	10.1561280000	2.3633820000	3.6201180000
S	9.4498810000	4.3527100000	4.5236180000
C	7.7609210000	4.1235350000	4.9744970000
C	7.3164570000	4.6276900000	6.2012090000
H	7.9385890000	5.0225260000	6.8016520000
C	5.9789900000	4.5570060000	6.5492920000
H	5.6877300000	4.9156950000	7.3799180000
C	5.0679280000	3.9675320000	5.6978920000
H	4.1487110000	3.9322630000	5.9370590000
C	5.4956150000	3.4276690000	4.4939180000
H	4.8698710000	3.0000520000	3.9215470000
C	6.8369270000	3.5069880000	4.1174840000
C	7.2593700000	3.0240520000	2.7624870000
H	6.4566570000	2.7263890000	2.2653460000
H	7.6601450000	3.7800660000	2.2653460000
C	8.7047200000	1.5736370000	1.4282630000
H	7.9479100000	1.3229500000	0.8252930000
C	9.4406770000	2.8040970000	0.9454380000
C	9.2579980000	3.4067420000	-0.2868880000
H	8.6457690000	3.0468820000	-0.9179280000
C	9.9867310000	4.5431030000	-0.5771440000
H	9.8783830000	4.9830130000	-1.4119810000
C	10.8768230000	5.0354040000	0.3638030000
H	11.3882760000	5.8127840000	0.1740410000
C	11.0174430000	4.3909050000	1.5750750000
H	11.6259440000	4.7342280000	2.2176250000
C	9.7285580000	0.4763500000	1.5436350000
C	9.8803630000	-0.5580100000	0.6428300000
H	9.2935320000	-0.6512310000	-0.0982490000
C	10.9166670000	-1.4570010000	0.8536450000
H	11.0504140000	-2.1805260000	0.2526410000
C	11.7501380000	-1.2951440000	1.9374740000
H	12.4566180000	-1.9097890000	2.0969190000
C	11.5421780000	-0.2193700000	2.7925230000
H	12.1210870000	-0.1024410000	3.5369710000
C	7.6932320000	0.7456230000	3.5619550000
H	7.9875210000	-0.0995140000	3.1383600000
H	6.7036460000	0.7726960000	3.5453930000
C	8.1770730000	0.7968430000	4.9809540000
C	7.4539320000	0.2413210000	6.0237990000
H	6.6011220000	-0.1478070000	5.8668810000
C	7.9898510000	0.2602000000	7.2965470000
H	7.5086890000	-0.1141480000	8.0255560000
C	9.2282900000	0.8265510000	7.4997830000
H	9.6139180000	0.8414780000	8.3680250000
C	9.9005180000	1.3725600000	6.4257780000
H	10.7533280000	1.7663720000	6.5686610000
N	8.2411510000	1.9026180000	2.8090850000
N	10.3070010000	3.2845450000	1.8616820000
N	10.5509610000	0.6544500000	2.5985510000
N	9.3851040000	1.3639260000	5.1822240000
N	11.7721570000	2.6314110000	4.1845740000
O	12.3764463012	3.5320459695	3.7855400646

BP86 optimized $^3\{\text{FeNO}\}^8$ structure starting from Initial Guess A (${}^3\{3\}\text{-A}$):

Fe	10.31570212220416	2.41828675714340	3.63429127507644
S	9.44628690275445	4.43204005708264	4.59908917794136
C	7.81050817909626	4.04974191217283	5.08275517597384
C	7.37660105239048	4.34291629461831	6.40343490379908
H	8.10217699149052	4.79423410634692	7.09630993744038
C	6.07348603347894	4.05831627193309	6.82411567104355
H	5.77298488115859	4.29315941309352	7.85722966471826
C	5.14920051956393	3.4710359828476	5.93697426235242
H	4.12187717144714	3.25000307671824	6.26304482132885
C	5.55743983179086	3.17584401475980	4.62914863625625
H	4.84485929365941	2.71947723126308	3.92159449551022
C	6.87001525561891	3.44043730001552	4.19338768252239
C	7.29312114135175	3.07058636693732	2.80254473157763
H	6.39951298101336	2.82708772386403	2.17968991721833
H	7.83267321827025	3.92132048238006	2.33862146503890
C	8.70509842105840	1.58556687635717	1.42996765671613
H	7.87780894922428	1.33394118138955	0.72720123739636
C	9.47685883090657	2.79418497738300	0.92026391772758
C	9.29841430780688	3.37816453484145	-0.33835555647528
H	8.51429862477740	2.99599638614868	-1.00925430156617
C	10.12234358448634	4.44874314342941	-0.71596086685543
H	9.99999626372697	4.93317540365057	-1.69533609159939
C	11.10082900581289	4.89641496439885	0.19547350302316
H	11.77063671197070	5.73238407700055	-0.05256182035785
C	11.21092568970285	4.27515294714930	1.43978239871725
H	11.94595291972940	4.59899667090123	2.19216692420393
C	9.71174471999052	0.45731308526734	1.50235734611017
C	9.87141852505567	-0.51382412796735	0.50510969824172
H	9.17014640790289	-0.55039013345013	-0.34309339489842
C	10.93348381631583	-1.42518199968866	0.60830975209059
H	11.07823280572023	-2.20616396356214	-0.15284487941867
C	11.81171175556285	-1.31443137544289	1.70769980326119
H	12.65746909218806	-2.00664637579656	1.83231522777321
C	11.58531891467144	-0.31560085356601	2.65728991138438
H	12.23644954228677	-0.18587102802187	3.53514637508309
C	7.71136990620058	0.76935496080009	3.57037354303472
H	8.18399691760806	-0.15256216537081	3.17732408061952
H	6.61127650822867	0.65494707035832	3.45375808107862
C	8.07098557419859	0.92604629097747	5.03268546170244
C	7.17877632443387	0.61559606783594	6.07136554675847
H	6.15820625151977	0.28487390412141	5.83204989864682
C	7.59466958407137	0.77810705326308	7.39786833782631
H	6.90696017300339	0.5615335954810	8.22833989946150
C	8.89532925405246	1.25015514470407	7.64464141524093
H	9.26414700838289	1.40412593577295	8.66894193959883
C	9.72084470558238	1.54098075616350	6.55424966520791
H	10.73711539061196	1.94098795693051	6.68610716748275
N	8.22834326453648	1.91308675928916	2.79471505975538
N	10.41896754209991	3.24020591852645	1.79886213054612
N	10.55299123270671	0.55099147754753	2.56955895816638
N	9.32429393498766	1.37361049326077	5.27963237998293
N	11.87444284711623	2.72393400846436	4.19252509401718
O	12.82829546037314	3.44224867037214	4.23896471731771

BP86 optimized $^3\{\text{FeNO}\}^8$ structure starting from Initial Guess B (${}^3\{3\}\text{-B}$):

Fe	10.23910042097914	2.40096418373406	3.60367785748275
S	9.41614602582289	4.43068524840777	4.52284988288392
C	7.78833247591322	4.06093842779903	5.04394730609904
C	7.37352344253500	4.37219862366393	6.36565359822767
H	8.10761763633012	4.83320241057551	7.04304813723208
C	6.07559689380429	4.09206724286270	6.80614091441025
H	5.78714907168046	4.34119027346338	7.83924024918320
C	5.14230684474668	3.48905031627208	5.93940532732077
H	4.12015167550790	3.26953042614687	6.28222620077907
C	5.53336086810271	3.17525963512555	4.63041147202978
H	4.81270844395486	2.70655572096307	3.93941233057264
C	6.83884132545716	3.43910219155172	4.17434839422863
C	7.25187868236005	3.05620352561655	2.78459273521072
H	6.35706354385798	2.78993072382531	2.17380551572176
H	7.77647337235122	3.90641080585114	2.30229242183251
C	8.67988669414713	1.57896236415092	1.41609697374878
H	7.85287178172968	1.33145945706555	0.71291552004541
C	9.45756000811495	2.78711924228002	0.91852835628965
C	9.28905654431778	3.38921248062182	-0.33297982302768
H	8.50225124723680	3.02323589890317	-1.00972975054393
C	10.12601985439064	4.45365899095501	-0.69668311688246
H	10.01188029738726	4.95030152706355	-1.67088491368142
C	11.10797160847286	4.87965238126872	0.22263451481847
H	11.79154995026920	5.70710620843625	-0.01578369566002
C	11.20616396508014	4.24701254805732	1.46180796116040
H	11.94315971234747	4.55234129429229	2.21964570088510
C	9.68793260758720	0.45720817339101	1.49589694685368
C	9.89498820691113	-0.49234364908557	0.48692067805815
H	9.21554729603012	-0.52818015057627	-0.37884287500823
C	10.97318083559298	-1.38243431109496	0.60098274782952
H	11.15319784721042	-2.14786737591487	-0.16806626018527
C	11.82447052899384	-1.26810549423573	1.72449069444900
H	12.68065279928612	-1.94512123075339	1.85998450702872
C	11.55664707517178	-0.29042229009408	2.68294313041226
H	12.18501724646166	-0.15998378370776	3.57670231372099
C	7.69761788069878	0.76627998818497	3.57081941646491
H	8.16263893502513	-0.15576060829866	3.16820524535876
H	6.59610815427811	0.65448791068722	3.47131025355720
C	8.08075582908332	0.93571515862770	5.02352448069015
C	7.21648495242961	0.61701856136186	6.08222526554790
H	6.19802446782904	0.26556467659172	5.86443742406987
C	7.65572822824780	0.79176900851908	7.39957594946608
H	6.9893232500285	0.56547818750266	8.24450496745563
C	8.95339590508704	1.28823940295959	7.61759971402761
H	9.34219481216695	1.44920969000720	8.63334258831472
C	9.74972757265339	1.59453461435414	6.51107224276524
H	10.75993257343179	2.01601067605662	6.61844083181529
N	8.20445234363100	1.91133082305725	2.78473833791656
N	10.40196257111190	3.21640430706148	1.80727008816854
N	10.50392200658281	0.55441511813703	2.58774570823583
N	9.33072931679684	1.41507188396935	5.24406302038206
N	11.80006076344368	2.69342042062912	4.17027810711312
O	12.76659360735704	3.39744314821002	4.14149040512462

BP86 optimized $^1\{\text{FeNO}\}^8$ structure starting from Initial Guess B ($^1\{3\}\text{-B}$):

Fe	10.18033992216995	2.38986676040849	3.49976361874097
S	9.47817929932052	4.33095833907516	4.54754739678785
C	7.81309163992219	4.01983880833432	5.00811981716261
C	7.40089330473246	4.31516802135163	6.33377740031404
H	8.14699056383325	4.73694942038620	7.02356392959764
C	6.09808461340726	4.05115283054643	6.77070030947979
H	5.81709617942760	4.27965968054363	7.81059707822683
C	5.15377782079397	3.48506659784068	5.89258257322123
H	4.12913536174094	3.27199699015144	6.23186559703873
C	5.53773205543975	3.20255207825121	4.57399409825148
H	4.80603207437553	2.77050303319500	3.87080331692728
C	6.84591566003576	3.45635660912925	4.11918240845751
C	7.23269853459322	3.10607043820283	2.70962851982344
H	6.32095556861002	2.88611320359830	2.10440232824382
H	7.77102276351456	3.95726924348528	2.24572122996260
C	8.69431041249075	1.63729850498671	1.32807545044242
H	7.91404757014092	1.37702790126361	0.57711627189103
C	9.48159228745770	2.85861865557047	0.87857582863751
C	9.38027043065651	3.45247856256745	-0.38139503274282
H	8.67690750241536	3.04066714105033	-1.12030049544061
C	10.16450262768814	4.58208976422518	-0.66899363853364
H	10.09753916955704	5.07701027919927	-1.64860462628836
C	11.02457285885681	5.07004999626387	0.33224098703391
H	11.65018609386905	5.95775939917368	0.16089024788077
C	11.08863068738898	4.42057981698151	1.56706178048344
H	11.75657264637868	4.73020475535064	2.38474073979990
C	9.69255816472496	0.51337277760236	1.49339750748534
C	9.78542748733934	-0.62990509833932	0.69523159175327
H	9.07484961755036	-0.77586103464147	-0.13211407498102
C	10.78822792847744	-1.57522606236640	0.97710426109204
H	10.88309332295634	-2.48824999948173	0.37175313879138
C	11.65819551875058	-1.33029201488494	2.05627842717879
H	12.45489506456901	-2.04268239752095	2.31568506838937
C	11.50855138181126	-0.16361592404094	2.81151776441361
H	12.15872457211763	0.10148525231759	3.65919807222887
C	7.65987111627951	0.80492435321598	3.46967726864197
H	8.07612984465035	-0.12879582504255	3.04254523864507
H	6.55269548896031	0.71219142500194	3.43377052826931
C	8.12967810421845	0.92681393719637	4.90689264864467
C	7.34407403651263	0.53228966254967	5.99774675782497
H	6.32425483464536	0.16180675736314	5.82335813629038
C	7.85863327662744	0.66367676076839	7.29519845062914
H	7.247292655564879	0.39013770673034	8.16734405017941
C	9.15803337006175	1.16894325958100	7.45640751602813
H	9.60504294676876	1.29333744613211	8.45316501527024
C	9.88401459757496	1.54232807487317	6.32088416931870
H	10.90154154250201	1.95716445454401	6.36730561927929
N	8.15291663386230	1.94395862249666	2.67899297679031
N	10.33428494120860	3.32941469835559	1.83970342275020
N	10.54338353165994	0.74409060164525	2.53491920920434
N	9.37892708987433	1.42777280536007	5.07688644566879
N	11.79124389868920	2.50437993857087	4.19340077629184
O	12.56229138314138	3.43596799088122	4.04036887852220

BP86 optimized $^2\{\text{FeNO}\}^7$ structure (starting from $[\text{Fe}(\text{NO})(\text{N3PyS})]^+$ X-ray structure):

Fe	10.13855044780028	2.40582545763293	3.53137559612425
S	9.42299788264795	4.38057724918954	4.48736156635303
C	7.78252576631780	4.02565488592943	5.01452257569270
C	7.39842501889653	4.30483030628041	6.34663493687012
H	8.14560122697359	4.72782459028874	7.03377617218189
C	6.09441201128468	4.03760106747729	6.78590968269728
H	5.81535395183931	4.26225263907924	7.82629441701191
C	5.14712711472364	3.48176294595900	5.90685432090252
H	4.12359130228166	3.27336703452354	6.25078799380349
C	5.51683406057792	3.20118875372834	4.58280295955822
H	4.77745565397157	2.77501580043183	3.88520122267083
C	6.82168135014424	3.46376357224345	4.12647503448869
C	7.23378113368125	3.12180272820884	2.72508566128258
H	6.34927339132494	2.85310974312414	2.10657432644386
H	7.75421322070227	3.98341774806704	2.26148161866443
C	8.69050642986085	1.64497163376629	1.34551155157722
H	7.87559457713094	1.38869063627828	0.63617175806952
C	9.47467969602256	2.85697186719598	0.87267653059648
C	9.39302173413176	3.42497840300603	-0.40061973685981
H	8.68946615535983	3.01657825593266	-1.14008443396354
C	10.21217736473559	4.52519639459502	-0.70236000754907
H	10.16545815553878	4.99928705094222	-1.69332151072411
C	11.07799151896147	5.01590764054083	0.28722545364026
H	11.72872911431611	5.88114328362182	0.09900677883198
C	11.10153872306522	4.40118830195494	1.54409725556230
H	11.75044298848477	4.75681598861087	2.35578827043241
C	9.68381964393492	0.51108943593137	1.49414542077836
C	9.78748769739838	-0.60741920599589	0.66291966424178
H	9.08565550985344	-0.74091116518354	-0.17327900154662
C	10.79950654962624	-1.54699515194803	0.92561378162994
H	10.90870230368638	-2.43933040808691	0.29224333843035
C	11.66350063312277	-1.32972975500137	2.01176462191988
H	12.46779601820070	-2.03983479321383	2.25087878034240
C	11.49294921321567	-0.18707159625753	2.80250815069459
H	12.13603283786498	0.03465061706363	3.66554825266448
C	7.67037892251215	0.82511022504605	3.49741439682341
H	8.07492667077845	-0.11292739894935	3.06956628040510
H	6.56517703006417	0.76256417438162	3.43399943763590
C	8.12183976700557	0.93997320054415	4.93417602807738
C	7.34650268334767	0.50803812530106	6.01707109403694
H	6.33732365432887	0.11254553013089	5.83823087211620
C	7.86243994400661	0.62099559360877	7.31483427518726
H	7.26321206872000	0.30680530818119	8.18119926897222
C	9.14935289582432	1.15336175725281	7.48739337986460
H	9.59609615802764	1.26329776562868	8.48534269768311
C	9.86300873506689	1.5728473454344	6.36182891685825
H	10.85920953469854	2.02730416359288	6.43820266613179
N	8.19949020209187	1.97513188616824	2.71919738824834
N	10.32433501113885	3.33608002151127	1.82224356458782
N	10.52412774611139	0.71274365826679	2.54140633404571
N	9.35901187050315	1.46826077269844	5.11611123366284
N	11.71506563400665	2.69878835738137	4.12521364925627
O	12.63153107408815	3.44764116879510	4.10727151289229

BP86 optimized $^4\{\text{FeNO}\}^7$ structure (starting from $[\text{Fe}(\text{NO})(\text{N3PyS})]^+$ X-ray structure):

Fe	10.27189870393919	2.54591556639687	3.72059836125231
S	9.49635689917983	4.41444045301867	4.72917984656206
C	7.81395626315118	4.05445610216578	5.11454051156817
C	7.37232222949688	4.31612258677321	6.43286928185539
H	8.08716663483883	4.73577714071095	7.15565076994690
C	6.05245589788240	4.04255285355925	6.81494445615634
H	5.73069260126130	4.25246955720245	7.84589065207483
C	5.14146049533137	3.51424049249323	5.88347855228016
H	4.10083823280579	3.31101100582475	6.17543204965102
C	5.56944193384872	3.25459332822018	4.57301195228902
H	4.85847996825323	2.84646540369957	3.83634727139489
C	6.89654473547999	3.50395401087658	4.17543104929122
C	7.34444461598153	3.15586119337445	2.78316780466375
H	6.46359514963799	2.91036628745049	2.14851912668979
H	7.87792364405212	4.01117120872413	2.32572160348356
C	8.75005798271901	1.63904218474744	1.42383602735152
H	7.91015184370952	1.34444988616739	0.75704467081901
C	9.48045303244589	2.84565426955733	0.85163968256552
C	9.29414652486558	3.34684583690144	-0.44091477428978
H	8.55532458290843	2.88724789778972	-1.11331756077989
C	10.06076027679717	4.45191352097397	-0.84659793426156
H	9.93541844517276	4.87527697469214	-1.85385075907377
C	10.97765380912842	5.01355840795888	0.05490772036739
H	11.59002282837776	5.88365708447903	-0.22043254044455
C	11.0943923472067	4.45026041285428	1.3325748045794
H	11.79368608923778	4.86043430640774	2.08145433170355
C	9.76335874379678	0.50876462039195	1.53232917325335
C	9.84327138356458	-0.56412072454594	0.63535505596084
H	9.12138640381586	-0.65757907960825	-0.18986953540269
C	10.86034035214329	-1.51576303247854	0.82129058401780
H	10.94810299060977	-2.37489182719014	0.13951536610784
C	11.75781168012733	-1.35784732714541	1.88901699636032
H	12.56475847129996	-2.08261465194967	2.06875967488900
C	11.60733692836689	-0.24831180296760	2.73388876386574
H	12.28202303867591	-0.06764592499481	3.58461845134287
C	7.72173454187432	0.84455115136061	3.53841377803121
H	8.14623045269287	-0.08788237522693	3.11745887232662
H	6.62032505296515	0.78491541499962	3.41649836331179
C	8.09431855206168	0.91954813140628	5.00092405819496
C	7.20821207962713	0.56459846074805	6.02883967458743
H	6.17818474379683	0.26909286475492	5.78537199948571
C	7.65044510489447	0.62358695237583	7.35605385882562
H	6.97011069721800	0.36736050114391	8.18098791032836
C	8.97054176280693	1.02759617323813	7.61508980354621
H	9.35981028160198	1.09006100876330	8.64098809295662
C	9.79040742888934	1.36851898294415	6.53582585482219
H	10.82260152915335	1.71675591034038	6.68424223540529
N	8.28991825478073	1.99577950228362	2.79238895790927
N	10.37127312062336	3.38773374004726	1.70814968955106
N	10.63379545024951	0.65564739552584	2.55222551059430
N	9.36148721245693	1.31615275830124	5.25979208569966
N	11.89908863525095	2.89338499629971	4.12712249217320
O	12.80834245143273	3.63760520816259	4.20187119828063

References:

- (1) Arulsamy, N.; Bohle, D. S.; Imonigie, J. A.; Sagan, E. S. *Inorg. Chem.* **1999**, *38*, 2716.
- (2) Armarego, W. L. F.; Perrin, D. D. *Purification of Laboratory Chemicals*, 4th ed.; Butterworth-Heinemann: Oxford, 1997.
- (3) Schopfer, M. P.; Mondal, B.; Lee, D. H.; Sarjeant, A. A.; Karlin, K. D. *J. Am. Chem. Soc.* **2009**, *131*, 11304.
- (4) Clark, M. M.; Brennessel, W. W.; Holland, P. L. *Acta Crystallogr., Sect. E: Struct. Rep. Online* **2009**, *65*, m391.
- (5) McQuilken, A. C.; Jiang, Y.; Siegler, M. A.; Goldberg, D. P. *J. Am. Chem. Soc.* **2012**, *134*, 8758.
- (6) Widger, L. R.; Jiang, Y.; McQuilken, A. C.; Yang, T.; Siegler, M. A.; Matsumura, H.; Moënne-Locoz, P.; Kumar, D.; de Visser, S. P.; Goldberg, D. P. *Dalton Trans.* **2014**, *43*, 7522.
- (7) McQuilken, A. C.; Ha, Y.; Sutherlin, K. D.; Siegler, M. A.; Hodgson, K. O.; Hedman, B.; Solomon, E. I.; Jameson, G. N. L.; Goldberg, D. P. *J. Am. Chem. Soc.* **2013**, *135*, 14024.
- (8) Evans, D. F.; Jakubovic, D. A. *J. Chem. Soc., Dalton Trans.* **1988**, 2927-2933.
- (9) Praneeth, V. K.; Paulat, F.; Berto, T. C.; George, S. D.; Nather, C.; Sulok, C. D.; Lehnert, N. *J. Am. Chem. Soc.* **2008**, *130*, 15288.
- (10) Praneeth, V. K.; Nather, C.; Peters, G.; Lehnert, N. *Inorg. Chem.* **2006**, *45*, 2795.
- (11) Goodrich, L. E.; Paulat, F.; Praneeth, V. K.; Lehnert, N. *Inorg. Chem.* **2010**, *49*, 6293.
- (12) Neese, F. *WIREs Comput. Mol. Sci.* **2012**, *2*, 73.
- (13) Grimme, S.; Antony, J.; Ehrlich, S.; Krieg, H. *J. Chem. Phys.* **2010**, *132*, 154104.
- (14) Grimme, S.; Ehrlich, S.; Goerigk, L. *J. Comput. Chem.* **2011**, *32*, 1456.
- (15) Weigend, F.; Ahlrichs, R. *Phys. Chem. Chem. Phys.* **2005**, *7*, 3297.
- (16) Schäfer, A.; Horn, H.; Ahlrichs, R. *J. Chem. Phys.* **1992**, *97*, 2571.
- (17) Pettersen, E. F.; Goddard, T. D.; Huang, C. C.; Couch, G. S.; Greenblatt, D. M.; Meng, E. C.; Ferrin, T. E. *J. Comput. Chem.* **2004**, *25*, 1605.
- (18) Ye, S.; Geng, C. Y.; Shaik, S.; Neese, F. *Phys. Chem. Chem. Phys.* **2013**, *15*, 8017-30.
- (19) Speelman, A. L.; Lehnert, N. *Angew. Chem. Int. Ed. Engl.* **2013**, *52*, 12283.
- (20) McQuilken, A. C.; Matsumura, H.; Durr, M.; Confer, A. M.; Sheckelton, J. P.; Siegler, M. A.; McQueen, T. M.; Ivanović-Burmazović, I.; Moënne-Locoz, P.; Goldberg, D. P. *J. Am. Chem. Soc.* **2016**, *138*, 3107.